Journal of Chromatography A, 1218 (2011) 1915–1938

Contents lists available at ScienceDirect

Journal of Chromatography A

journal homepage: www.elsevier.com/locate/chroma

Review

Shell particles, trials, tribulations and triumphs

Georges Guiochon[a,b,*], Fabrice Gritti[a,b]

[a] Department of Chemistry, University of Tennessee, Knoxville, TN 37996-1600, USA
[b] Division of Chemical and Analytical Sciences, Oak Ridge National Laboratory, Oak Ridge, TN 37831-6120, USA

ARTICLE INFO

Article history:
Available online 23 February 2011

Keywords:
Column efficiency
Corasil
Halo
Kinetex
Pellicosil
Pellicular particles
Permaphases
Poroshell
Shell particles
Superficially porous particles
Zipax

ABSTRACT

The concept of pellicular particles was imagined by Horváth and Lipsky fifty years ago. They were initially intended for the analysis of macromolecules. Later, shell particles were prepared. The rational behind this concept was to improve column efficiency by shortening the pathways that analyte molecules must travel and, so doing, to improve their mass transfer kinetics. Several brands of superficially porous particles were developed and became popular in the 1970s. However, the major improvements in the manufacturing of high-quality, fully porous particles, that took place in the same time, particularly by making them finer and more homogeneous, hampered the success of shell particles, which eventually disappeared. Recently, the pressing needs to improve analytical throughputs forced particle manufacturers to find a better compromise between the demands for higher column efficiency that require short diffusion paths of analyte molecules in columns and the need for columns that can be operated with the conventional instruments for liquid chromatography, which operate with moderate column back-pressures. This lead to the apparition of a new generation of columns packed with shell particles, which bring chromatographic columns to a level of efficiency undreamed of a few years ago. This evolution is reviewed, the reason that motivated it, and the consequences of their success are discussed.

Contents

* Corresponding author at: Department of Chemistry, University of Tennessee, Knoxville, TN 37996-1600, USA. Tel.: +1 865 974 0733; fax: +1 865 974 2667.
E-mail address: guiochon@utk.edu (G. Guiochon).

0021-9673/$ – see front matter © 2011 Elsevier B.V. All rights reserved.
doi:10.1016/j.chroma.2011.01.080

1. Introduction

The early beginnings of modern liquid chromatography were uncertain, difficult, and patchy. The concept of high pressure liquid chromatography, which later became high performance liquid chromatography (HPLC) was born at about the same time in the minds of many specialists of gas chromatography. In this earlier, more advanced analytical technique, the flow of mobile phase is tightly controlled while sample injection and the detection of the separated components are done on-line. It was tempting to extend this analytical procedure to column liquid chromatography, which was still most empirical in the mid-1960 and was practiced in the same way as Tswett was used to [1–3]. Scientists working in gas chromatography had been very successful in developing an efficient, powerful, accurate method of analysis for vapors, including a wide range of hydrocarbons, petrochemicals, fine chemicals, fats and many derivatives of hydroxylated compounds. However, gas chromatography could not be extended to many compounds of importance in the life sciences and analysts were frustrated. They turned toward liquid chromatography. Developing instruments similar to those used in gas chromatography was not a major obstacle and this required only a few years [4]. However, preparing suitable stationary phases was a major roadblock. Three avenues were explored: ion-exchange, liquid–liquid, and liquid–solid chromatography.

The idea of using thin films of ion-exchange polymers coated on solid particles or on the surface of particles with small specific surface area was in the air in the late 1960s. Parish suggested using beads of cross-linked polystyrene bearing ion-exchange groups in a shallow surface layer to separate metal ions [5]. Knox recommended the use of thin films of the stationary liquid phase in liquid–liquid chromatography (LLC) [6]. Horváth and Lipsky suggested the use of pellicular (i.e., thin-skin) particles instead of fully porous particles as packing materials for chromatographic columns and demonstrated the value of the concept by reporting important analytical results in the ion-exchange analysis and/or the purification of nucleosides [7,8]. The rational of these inventors was that columns packed with such particles would have a higher efficiency than those packed with fully porous particles because diffusion through the thin porous layer surrounding the particles would be faster than diffusion through the whole particles. This acceleration of diffusion would reduce the time required for solute equilibration between the monolayer on the surface of the mesopores of the particles and the mobile phase or, more exactly, would effectively reduce the resistance to mass transfer through the stationary phase. This idea made sense at a time when the average particle size of the packing materials was ca. 80 μm. The initial experimental work was based the use of ion-exchange as the retention mechanism [5,7]. This mechanism was applicable only to a restricted number of compounds, insufficient to justify the development of a new major analytical method. A more general approach was required.

At about the same time and for the same reason, shell (i.e., thick-skin) particles were prepared by Kirkland and used extensively for the analysis of macromolecules and particularly of proteins [9–11]. The spherical shape and the greater mechanical strength of these particles would result in a higher column stability and a better reproducibility than those of columns packed with the irregularly shaped silica particles popular in early times and used to separate mixtures of hydrocarbons. These new packing materials were called controlled surface porosity supports [9,10]. They were designed to be suitable for the implementation of LLC.

Because gas chromatography used as stationary phase a liquid spread over the surface of a tube or of an inert support (and was, therefore, called gas–liquid chromatography or GLC), the first approach to be intensely investigated by analysts coming from the GLC field was liquid–liquid chromatography In the late 1960s, the 1970s, and the early 1980s, Huber [12,13], Halasz et al. [14], and Karger and Berry [15] actively pioneered the use of LLC. This was why 30–50 μm shell particles were made, with a solid glass bead core, similar to the beads used by Horváth et al., but which were surrounded by a ca. 1 μm thin layer of fine silica particles. The particles prepared by Kirkland had been designed for this purpose and were widely used. Sold under the name Zipax (Dupont de Nemours, 1970), it was the most popular among the brands of these shell particles which were produced in the early 1970s, including the 37–50 μm Corasil I and II (Waters Associates, 1970) and the 50 μm Pellicosil (Macherey-Nagel, 1975) [11,16]. The porous layer was impregnated with a liquid serving as the stationary phase. The volume fraction of the particle occupied by the porous shell was between 5 and 10% and the minimum reduced HETPs of the columns packed with them was between 2.0 and 2.5 [17,18]. However, it rapidly proved more difficult than anticipated to find two liquids practically insoluble in each other and between which the sample components would equilibrate with constants different from either zero or infinity. Furthermore, it was realized that LLC columns were unstable, rapidly losing stationary phase and providing irreproducible analyses. The use of liquid stationary phases was abandoned in favor of adsorbents.

As a first approximation, the column efficiency is inversely proportional to the average size of the particles of the packing media used to fill the column. This explains why the most important, persistent trend in the development of HPLC over the last forty years has been the development of methods for the manufacturing of packing materials made of particles of decreasing average size and better packing characteristics. The average size of the particles used to pack HPLC columns was initially in the 100 μm range [19,20]. Later, this average size decreased progressively to 40–50 [4,21], then to 20, 10 [20], and 5 μm, a range that was already reached in the early 1980s and remained nearly unchanged until the turn of this century, in spite of the availability of 3 μm and even smaller 1 μm particles [22]. The only major change that took place in the 1980s and 1990s was the development of spherical particles that eventually came to dominate entirely the market of packing materials.

Then, under the combined pressures of the requirements by the pharmaceutical and fine chemicals industries for accelerated analytical throughputs and the threats of the monolithic columns that were commercialized in 2000 with great expectations, the man-

ufacturers of packing materials capitalized on their experience in the production and packing of regular, spherical, reproducible 5 μm particles [23–28] and rapidly began to commercialize columns packed with 3, then 2, and now with the sub-2 μm particles, which have average sizes between 1.5 and 1.7 μm. Finer particles, with average size of 1 μm are already available for nearly ten years but with limited commercial success because these are solid, non-porous particles [22]. Then, a few years ago, the concept of shell particles was suddenly revived to an amazing success [29–31].

The goal of this paper is to review the origin, purpose, development and properties of columns packed with type of particles and to explore their perspectives. The structure of the particles has considerably evolved over the nearly fifty years over which they have been successively tried, abandoned, then successfully rediscovered. So did the names used for them. As pointed out by the reviewers, it is not possible to be fully consistent and use the same name for commercial products of different structures, made at different times. Initially, these particles were called *pellicular* or *s* uperficially porous particles because it was felt that a very thin layer of porous material around large solid cores would exhibit a low mass transfer resistance and allow the production of high column efficiency. The first term disappeared because it implies a very thin porous layer of retentive material on a solid core, a material that would provide too small a saturation capacity to be useful in practical applications. The second term survives [31]. Later, the names of *controlled porosity materials (CPM)* or *f* used core particles were used by different manufacturers. They seem to have been abandoned. Finally, the names of *core–shell* or , for short, *shell* particles are becoming universally accepted. In this review, we will try and stick to the original names of the historical materials and use core–shell particles for all modern materials.

2. Theory

We compare in this section the properties of columns packed with fully porous, shell, and pellicular particles. To draw realistic conclusions, we need to compare data obtained with these different columns (see next section).

2.1. Influence of the shell thickness on the retention times and the saturation capacity of the column

To better understand the nature of the problems encountered in the manufacture and use of, pellicular, superficially porous and shell silica particles and the evolution of these problems over the years, some simple geometrical considerations are useful. The volume of the porous shell surrounding a particle is $\pi(d_e^3 - d_i^3)/6$, where d_e and d_i are the diameters of the particle and of its solid core, respectively. The volume fraction of the porous material, i.e., of the shell in the column is $(d_e^3 - d_i^3)/d_e^3 = 1 - (d_i/d_e)^3$. When the layer of porous material around the solid core is thin, this fraction becomes close to $3(1 - (d_i/d_e))$. When the thickness of this layer becomes significant, the volume fraction of porous material in the particle becomes large and eventually tends toward unity. For example, for the Halo particles (d_e = 2.7 μm, d_i = 1.7 μm), the shell thickness is 0.5 μm and for the Kinetex particles (d_e = 2.6 μm, d_i = 1.9 μm), the shell thickness is 0.35 μm. The volume fractions of the porous shells in these particles are 75 and 63%, respectively. Fig. 1 illustrates this relationship, the relative shell thickness being $e = (d_e - d_i)/d_e$. The shells of the superficially porous, also named pellicular, particles had a relative thickness, *e* well below 0.1 and an absolute thickness below 1 μm [8] for diameters of the order of 50 μm. This difference explains their markedly different properties and why these two types of columns must be considered separately.

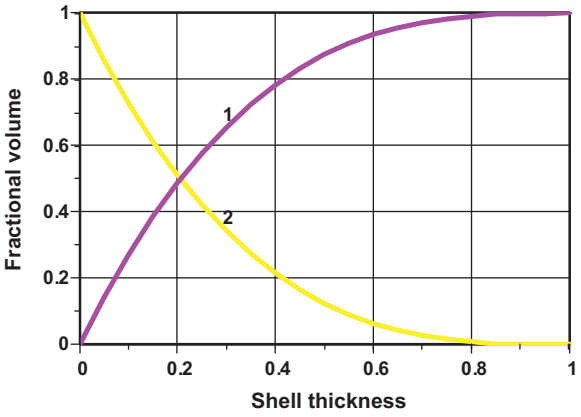

Fig. 1. Fractional volumes in the core–shell particles as a function of the relative shell thickness *e* (see text). 1, fractional volume of the shell; 2, fractional volume of the core.

The most important difference between the characteristics of columns packed with core–shell and with superficially porous particles is in their hold-up times, retention factors, and saturation capacities. Because the volume fraction of the stationary phase in superficially porous particles is much lower than that of core–shell particles, the retention on columns packed with them tends to be lower or much lower than on columns packed with fully porous or even core–shell particles. This requests the use of lower concentrations of the strong solvent in the mobile phase and the injection of smaller amounts of samples into the column in order to do chromatography under linear or nearly linear conditions. This makes columns packed with superficially porous particles unsuitable for trace analyses. This explains also why columns packed with core–shell particles, for which the fractional volume occupied by porous silica remains close to that of columns packed with fully porous particles, are prospering while columns packed with superficially porous particles are not. Furthermore, although the layer of porous material around the particles is much thinner in superficially porous than in core–shell particles, the mass transfer resistance in the former is rarely much lower than in the latter (see Section 2.4.1), except for very thin porous layers and for very large molecules that diffuse in the most sluggish fashion, anyway. The reason for the failure of the shell concept is that mass transfer through particles is far from being the dominant contribution to band broadening in HPLC [32]. Yet, columns packed with these particles are tremendously successful, but for another reason.

2.2. Influence of the particle size on the column permeability

The permeability of a column or packed bed expresses the degree of resistance encountered by a stream of fluid forced to percolate through a porous bed. Whether the particles are porous or not, the fluid flows around and between the particles, not through them, except in some rare cases. The main obstacles encountered by the fluid stream along its path are the particles, the average size of which is the parameter that determines the bed permeability. It would be only if the particles were to have large through-pores, with diameters of the same order of magnitude as the particle diameter, that a secondary stream would significantly contribute to the overall flow rate. This situation has never been clearly established, so far. Admittedly, however, the shape of the particles and the smoothness of their external surface may contribute to some extent to the resistance they opposes to the stream [33]. It seems probable that the influence of the nature of the particle surface (e.g., its smoothness) on the permeability is indirect and results more from the friction between the particles and between the bed

and the internal surface of the column tube, because these frictions determine the external porosity of the packed bed and the packing density of the particles [34,35].

The flow of the mobile phase stream in a chromatographic column is relatively slow. Its Reynolds number is small, of the order of 1×10^{-3} to 1×10^{-2} [36]. For example, the mobile phase (acetonitrile) velocity in typical columns packed with 2.6 μm particles is of the order of $1–3 \times 10^{-3}$ m/s [37]. With $\rho = 0.7857$ at 20 °C and $\eta = 0.324$ cP at 30 °C, this gives $\mathrm{Re} \simeq 1.25 \times 10^{-2}$. So, the flow is laminar and follows Darcy law [38], which is written

$$u_0 = \frac{k_0 d_p^2 \Delta P}{\eta L} \tag{1}$$

where u_0 is the superficial velocity of the stream, d_p the average particle size, ΔP the difference between the inlet and outlet pressures of the column, η is the fluid viscosity, L the column length, and k_0 is the column permeability coefficient. Actually, the product $k_0 d_p^2$ is the column permeability. The permeability is also related to the external porosity of the bed, ϵ_e through the Kozeny–Carman equation [39].

$$k_0 d_p^2 = \frac{d_p^2}{180} \frac{\epsilon_e^3}{(1-\epsilon_e)^2} \tag{2}$$

The numerical coefficient (180) varies with the shape and the surface smoothness of particles [33], which might also affect ϵ_e.

Today, the finest core–shell particles available have a diameter of 1.7 μm. The earliest pellicular particles had diameters between 35 and 50 μm. So, the columns packed with these particles had a permeability that was more than a thousand times larger than that of columns packed with the new core–shell particles. Raising the mobile phase tank a few meters above the column inlet or using a peristaltic pump easily allowed a suitable mobile phase flow rate. With the current sub-2 μm particles, the maximum efficiency is obtained for mobile phase velocities of the order of

$$u_0 = 10 \frac{D_m}{d_p} = 5.9 \times 10^4 D_m \tag{3}$$

(with u_0 in cm/s) where D_m is the molecular diffusivity of the analyte, between 1×10^{-5} for small molecules and 1×10^{-7} for large biochemical compounds, including most of the biopharmaceuticals. This gives velocities between 0.6 and 6×10^{-3} cm/s.

2.3. Band broadening in chromatographic columns and the plate height equation

It is generally accepted that there are four sources of band broadening during the elution of a compound band [32,40,41]. Three of these sources originate in the column, the fourth one is due to the instrument itself [42–44]. These sources of band broadening in the column are the diffusion of the analyte molecules against the concentration gradient accompanying the band, the eddy dispersion due to the anastomosis and the unevenness of the flow stream structure, and the mass transfer resistances, due to the finite time that it takes for the mobile and the stationary phase to reach local equilibrium. As suggested by Giddings [40], the degree of band dispersion taking place in a column is characterized by the column HETP defined as the ratio of the increment of band variance to the increment of migration distance:

$$H = \frac{d\sigma^2}{dz} \tag{4}$$

There is a considerable amount of literature on the measurement of the HETP of a column, most of which reports experimental results of dubious precision and poor accuracy; a few papers only deal with the details of appropriate measurement processes and with accuracy and precision. The most serious disagreements observed between the different scientists involved arise from the tension between the desire of those experimentalists who want to follow a sound procedure that will provide theoretically exact values and the desires of those who want to achieve fast and precise measurements. Unfortunately, it seems most difficult to achieve both high accuracy and high precision and the debate remains open. We are of the opinion that accuracy is more important than precision [45].

Exact measurements require the integration of the elution band to measure its first three moments, giving the band area ($\mu_0 = A$), its thermodynamically correct retention time (μ_1, a value different from that of the elution time of the band apex if the profile is not symmetrical), and its variance (μ_2') that characterizes the peak spreading around the mass center of the band. These moments are given by the following equations

$$\mu_0 = \int C(t)dt \tag{5}$$

$$\mu_1 = \frac{\int C(t)t dt}{\int C(t)dt} \tag{6}$$

$$\mu_2' = \frac{\int C(t)(t-\mu_1)^2 dt}{\int C(t)dt} \tag{7}$$

Then, the integration of the mass balance of the general rate model of chromatography under linear isotherm conditions shows that the column HETP is given by

$$H = \frac{L}{N} = \frac{\sigma^2}{t_R^2} L = \frac{\mu_2'}{\mu_1^2} L \tag{8}$$

This value is easy to derive and the data stations of most instruments are programmed to provide it. It would be cautious, however, to validate the data provided by these data stations [46]. It is easy to download the detector signal into a spreadsheet and calculate the moments from this table [45]. The main obstacle reside in the limited precision of the measurements, which is due to the very definition of high-order moments. The higher the moment order, the heavier the weight of the sides of the band in its determination [41,47]. Accordingly, the signal noise limits the precision that can be achieved for the accurate value of the HETP.

The alternate method preferred by many experimentalists assumes that the profile of the elution peak is Gaussian and derives the column HETP from the band width at a fractional band height, usually the band width at half-height, with

$$H = 5.54 \left(\frac{t_R}{w_{1/2}} \right)^2 \tag{9}$$

Because the slope of the band is high near its half-height, the determination of the corresponding band width is precise, even for moderate values of the signal/noise ratio in excess of ca. 20. Unfortunately, the result of this method is most seriously inaccurate [45]. Due to a variety of diffusive phenomena taking place in the device used to inject the sample, the profile of the injected bands when they enter the column are often close to an exponential decay and differ considerably from a Dirac-δ or even a rectangular profile [41,44].

We prefer the moment method and use it unless small sample sizes must be injected and the signal to noise ratio is low, making the accuracy of this method to become insufficient. Then the recorded elution profile may be fitted to a model, e.g., an exponentially modified Gaussian, for detailed studies of column efficiency which are made with low or moderate polarity compounds. The moments of the best-fit profile are then calculated. This method is far less accurate than the integration method [45].

The experimental data on the relationship between the column HETP and the mobile phase velocity could be fitted to the van Deemter equation

$$H = \frac{B}{u_0} + A + Cu_0 \tag{10}$$

The terms A, B, and C account for the contributions to band broadening of the eddy dispersion, the axial dispersion in the mobile and the stationary phase, and the mass transfer resistances, respectively. These depend on the characteristics of the phase system and of the column. Each of them is complex, being due to the combination of several effects [48].

2.4. Column efficiency and the mass transfer kinetics

The mass transfer resistance term is the sum of two coefficients, the external or film mass transfer coefficient, C_f, and the trans-particle mass transfer coefficient, C_p. The former accounts for the difficulties encountered by analyte molecules to penetrate into the network of mesopores inside the particles; the latter for the time that it takes for them to diffuse across this network, once they have entered into it. The Wilson–Geankoplis correlation [49] provides a convenient estimate of the film mass transfer coefficient , k_f

$$Sh = \frac{k_f d_p}{D_m} = \frac{1.09}{\epsilon_e^{2/3}} \nu^{1/3} \tag{11}$$

where Sh is the Sherwood number, d_p the average particle size, D_m the molecular diffusivity, ϵ_e the external porosity, and $\nu = ud_p/D_m$ the reduced interstitial linear velocity of the mobile phase. This correlation is based on the rate of dissolution of benzoic acid from 6 mm diameter spheres. Its validity for the mass transfer of analytes in liquid chromatography, with 50 μm porous silica particles has recently been demonstrated [50,51]. The corresponding contribution to band broadening is given by

$$h_{\text{film}} = \frac{1}{3} \frac{\epsilon_e}{1-\epsilon_e} \left[\frac{k_1}{1+k_1}\right]^2 \frac{1}{Sh} \tag{12}$$

where k_1 is the retention factor of the analyte. Remarkably, this contribution does seem to depend on the structure of the particles.

2.4.1. Influence of the shell thickness on the mass transfer resistance across the particles

The contribution to the mass transfer coefficient due to diffusion across porous particles is

$$C_p = \frac{1}{30} \frac{\epsilon_e}{1-\epsilon_e} \left[\frac{k_1}{1+k_1}\right]^2 \frac{D_m}{D_{\text{eff}}} \tag{13}$$

where D_{eff} is the diffusion coefficient in the porous medium, sum of the contributions of pore and surface diffusion [52,53]. The same rigorous expression of the C_p coefficient for pellicular particles was derived by Horváth and Lipsky [8], who used the Aris theory of diffusion in heterogeneous media, later by Kaczmarski and Guiochon [54] who used the algebraic solution of the general rate model, and recently by [55] who applied the stochastic theory of chromatography. This gives

$$C_p = \frac{1}{30} \frac{\epsilon_e}{1-\epsilon_e} \left[\frac{k_1}{1+k_1}\right]^2 \frac{1+2\rho+3\rho^2-\rho^3-5\rho^4}{(1+\rho+\rho^2)^2} \frac{D_m}{D_{\text{eff}}} \tag{14}$$

where ρ is the ratio of the radii of the core and of the particle (thus, $\rho = 0$ for fully porous particles and $\rho = 1$ for nonporous particles). The results of these derivations show that the ratio of the C_p coefficients of the columns packed with core–shell and fully porous particles is [32]:

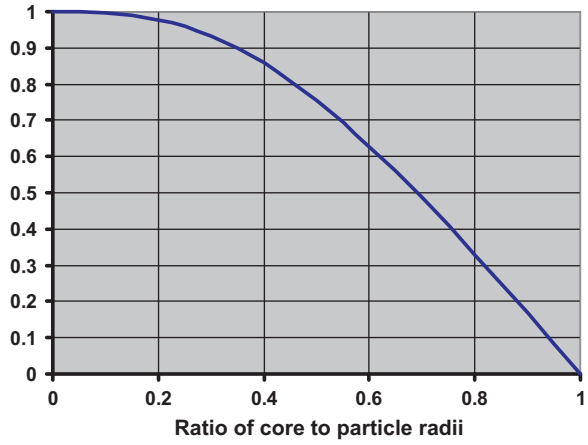

Fig. 2. Variation of the ratio, ΔC_p, of the mass transfer coefficients of a core–shell and a fully porous particle with the ratio of the core to the particle radii (see Eq. (15)).

$$\Delta C_p = \frac{C_{p,\text{shell}}}{C_{p,\text{fully porous}}} = \left[\frac{1+k_1-\rho^3}{1+k_1}\right]^2 \frac{1+2\rho+3\rho^2-\rho^3-5\rho^4}{(1+\rho+\rho^2)^2} \tag{15}$$

where k_1 is the zone retention factor, which also depends on the shell thickness and is given by [54]:

$$k_1 = \frac{1-\epsilon_e}{\epsilon_e} \left[\epsilon_{\text{shell},p} + (1-\epsilon_{\text{shell},p}) K_{\text{shell}}\right] (1-\rho^3) \tag{16}$$

where K_{shell} is the Henry constant for the adsorption-desorption equilibrium of the solute in the porous adsorbent and $\epsilon_{p,\text{shell}}$ is the porosity of the shell (generally of the order of 0.4). Obviously, K_{shell} is a function of the composition of the mobile phase, which could be altered to adjust the value of the zone retention factor, k_1.

The contribution of the first term in Eq. (15) is relatively unimportant for strongly retained compounds. When ρ increases from 0 to 1, it decreases from 1 to $[k_1/1+k_1]^2$. The variation of the second term in this equation is illustrated in Fig. 2. This term is still larger than 0.10 for $\rho = 0.94$. This shows that, although theoretically sound, the idea of preparing superficially porous particles with the purpose to increase the column efficiency by reducing the mass transfer resistance across the particles might provide only modest practical gains for the separation of low or medium molecular weight compounds.

2.5. Column and instrument contributions to band broadening

It is impossible to operate a column and measure its performance without fastening the column to an instrument. The process of operating the column affects the results achieved. The instrument contributes to the head pressure needed to force the required flow rate of mobile phase through the column and to the hold-up volume measured. Band dispersion takes place during the elution of the band through the injection device, the detector and the connecting tubes. Data acquisition may also affect the shape of the signal recorded. These contributions depend on the characteristics of the instrument [43,44]. Depending on the relative importance of the band broadening contributions of the instrument and of the column, the actual performance recorded may reflect the actual performance of the column, a combination of both the performance of the instrument and the column, or may be essentially due to the instrument.

The standard deviation σ_V in volume unit of a band at its elution from the column is given by

$$\sigma_V = \sigma_t u_0 \pi \frac{d_c^2}{4} = \frac{(1+k)L\pi\epsilon_T d_c^2}{4\sqrt{N}} \quad (17)$$

where σ_t is the band standard deviation in unit time, at the column exit, u_0 the superficial velocity of the mobile phase, ϵ_T the column total porosity, L the column length, k the retention factor of the analyte, H the column HETP, and d_c its diameter.

The relative importance of the instrument contribution depends very much on the dimensions of the column and on its performance. It is far less for strongly retained compounds than for early eluting ones. It is much less important in gradient elution than under isocratic elution. The large importance of this contribution was a very serious drawback to the development of HPLC in the 1970s. Progress in instrument design and construction during the late 1970s solved the problem for a whole generation. Recent progress in column technology and particularly the development of fine sub 2 μm particles and of 1.7 and 2.6 μm core–shell particles has resulted in the use of much smaller columns. The HETP of the columns packed with these new particles is smaller than that of conventional columns packed with 5 μm particles, which were the staple of HPLC during more than 25 years; so, columns can now be shorter and they are faster. However, their permeability being lower than that of the conventional columns, they must be operated under higher pressure gradients and the viscous friction of the mobile phase percolating through the column bed is generating a significant heat power. The use of narrow bore columns is required to restrict the consequences of this heat, which is generated across the column [56]. Therefore, modern columns must be short and narrow, which makes very small the variances of eluted bands. This evolution is making again critical changes in instrument design to drastically reduce the instrument band broadening [57].

3. Brief history of the development of pellicular and core–shell particles

This development of the superficially porous and the core–shell particles was chaotic, not progressive as that of the production and use of the finer and finer fully porous particles in HPLC. After the concept of superficially porous particles had been presented, it took time before reliable procedures for the preparation of pellicular first, then of core–shell particles be developed. Superficially porous particles are relatively easy to prepare [7,8,58]. However, the importance of their major inconvenience, their low saturation capacity, was realized rather early, which explains the early move toward core–shell particles, which appeared to be the rational solution to provide a compromise between high loading capacity and high efficiency. The production of high quality core–shell particles required considerable progress in silica chemistry and this progress came late, after numerous trials that took place over many years [11,16,31,59]. The eventual success came late but was as impressive as it should have been unexpected: the major progress that the advent of core–shell particles is bringing to column technology is not due to the shortening of the residence time of analyte molecules in the porous layer of the stationary phase particles but to the surprising mechanical properties of the particles, due in part to their narrow size distribution and, possibly, to the surface properties of the porous layer, particularly the roughness of its surface.

3.1. The beginning

The concept of pellicular particles was initially suggested by Horváth et al. [7,8] who reported on the preparation of such columns for ion exchange chromatography. They expected two advantages: (1) a high loading capacity due to the large saturation capacity of ion-exchange resins and (2) a low solid–liquid mass transfer resistance, due to the thin stationary phase layer [8,54].

Horváth et al. [7,8] prepared spherical glass beads (between ca. 50 and 100 μm in diameter), coated with a thin film of styrene, divinylbenzene and benzoyl peroxide, possibly a few μm thick. The film was polymerized and cross-linked at 90 °C. Then, classical organic chemistry reactions made on the aromatic rings of the coating were used to bind to them sulfonic acid or quaternary ammonium ions, providing strong cation or anion exchangers. The particles were packed into 1 mm I.D. stainless steel tubes, 1–2 m long. These columns were eluted in gradient elution mode. An example of the results reported by Horváth et al. [7] is provided in Fig. 3. The 1.93 m long anion-exchange column was eluted at a flow rate of 1 cm/s (inlet pressure, ca. 35 bar) with an ammonium formate buffer. This velocity corresponds approximately to a reduced velocity of 6000 for an unretained tracer. Depending on the retention factors of the ribonucleosides analyzed, the efficiency was of the order of 250–300 theoretical plates (H = 0.35 cm), corresponding to a reduced HETP of ca. 70. A 90 min salt gradient gave a peak capacity of the order of 15. No systematic attempt at operating the columns at much lower velocities was reported. Later results suggest that the efficiency would have been markedly improved but no analyst would be ready to wait for the days that elution would have required.

In spite of the impressive separations reported by Horváth et al., this type of stationary phase was not adopted by the community, mostly because ion-exchange is a retention mechanism that is specific of ions. This mode of retention did not interest much the early

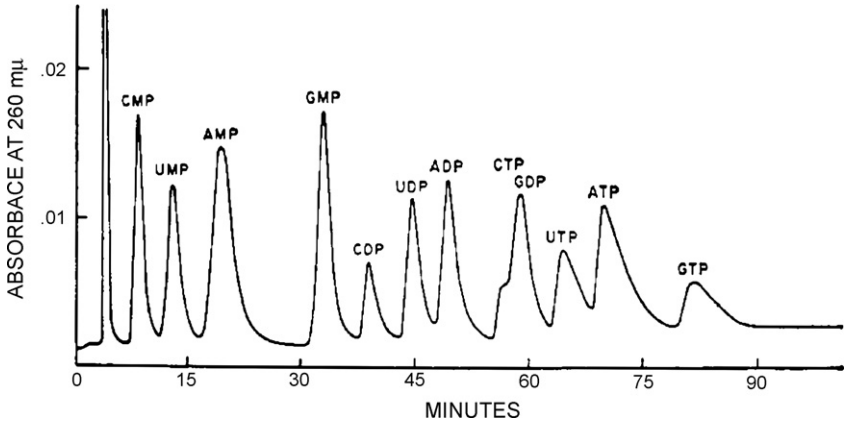

Fig. 3. Chromatogram of a mixture of ribonucleosides on a 193 × 0.1 cm column packed with 50 μm particles superficially coated with a film of an anion exchanger. Gradient elution, 0.04–1.5 M ammonium formate (pH = 4.35) at 1 cm/s hence ν = 5000 (=1100ν_{opt}, h = 80, N = 250 plates; peak capacity ¡15.

chromatographers who developed high performance liquid chromatography with experience, concepts and ideas derived from gas chromatography. Most of them preferred to develop liquid–liquid (LLC) rather than liquid–solid chromatography (LSC), due to the poor results generally obtained in gas–solid chromatography. It took time to get over this piece of conventional wisdom.

The HETP curves of these columns have a shape that would now seem unusual. Three regions can be distinguished in these curves. At high velocities, H increases linearly with increasing mobile phase velocity. At very low velocities, the classical van Deemter profile and its quasi-parabolic shape are observed. In the intermediate velocity range, a transition shape is observed, resembling a power function of the mobile phase velocity with an exponent lower than unity. This profile was observed typically in HPLC until particles below 20 μm in diameter became common.

3.2. Pellicular and micropellicular particles

Truly pellicular particles were prepared in 1986 by, Unger et al. [58] who reacted nonporous silica particles with an average size of 1.5 (±2%) μm with n-octyldimethyl chlorosilane, giving a layer of n-octyl bonded silica. No data on the carbon content, the specific surface area of the material, nor HETP data were provided. Note that the specific surface area of geometrical spheres of 1.5 μm diameter is 1.8 m^2/g, with a probable actual surface area for the particles used around 4–5 m^2/g. These particles were packed in 8 mm × 36 mm columns, which were used in gradient elution of acetonitrile, methanol or propanol in water with TFA. Mixtures of authentic proteins were separated with peak capacities between 20 and 40. Surprisingly, the slope, S, of the plots of the logarithm of the retention factors of proteins versus the organic modifier concentration was several times lower than usually observed with columns packed with fully porous particles.

Kalghatji and Horváth [60] demonstrated the use of 4.6 mm × 30 mm long columns packed with similar superficially porous 2 μm particles made of C_8 bonded solid silica beads for the separation of peptides by gradient elution (water/acetonitrile) at 80 ° C with flow rates of 4–5 ml/min. A peak capacity of ca. 35 was achieved in 200 s for the separation of the protein digest of methionyl human growth hormone. The sample size was 5 ng. Although rapid separations were achieved through the combined use of superficially porous particles and a high column temperature which provides fast mass transfer kinetics, this approach was not successful, due to the low saturation capacity of the column and to the limited thermal stability of the stationary phase at elevated temperatures.

3.3. The first generation of pellicular particles

Kirkland produced the first controlled-porosity particles [11] for liquid–liquid chromatography (LLC). These particles were made of spherical siliceous hard cores with a porous layer of controlled thickness and average pore size. These particles were coated with a liquid stationary phase, β, β'-oxydipropionitrile, and used to pack 50 cm long HPLC columns. The average particle size was 40 μm and the shell specific surface area was 0.83 m^2/g. The lowest HETP value, H = 0.11 mm (h = 2.7, was recorded at 0.02 cm/s (ν = 53), suggesting a minimum value of the order of 2. The column performance markedly exceeded that of a column packed with fully porous particles of diatomaceous earth, a conventional support used in GC at the time.

In the late 1960s and early 1980s, Huber [12,13], Halasz et al. [14], and Karger and Berry [15] actively pioneered the use of LLC. This was why, 40–50 μm pellicular particles were made, with a solid glass bead core, similar to the beads used by Horváth et al., which were surrounded by a ca. 1 μm thin layer of fine silica particles. This layer was impregnated with a liquid serving as the stationary phase. Several brands of these particles were produced in the early 1970s, including the 37–50 μm Corasil I and II (Waters Associates, 1970), the 50 μm Zipax (Dupont de Nemours, 1972), and the 50 μm Pellicosil (Macherey-Nagel, 1975) [11,16]. The volume fraction of the particle occupied by the porous shell was between 5 and 10% and the minimum reduced HETPs of the columns packed with them was between 2.0 and 2.5 [17,18]. However, it rapidly proved difficult to find two liquids practically insoluble in each other and between which the sample components would equilibrate with constants different from either zero or infinity. Furthermore, it was soon realized that LLC columns were unstable, rapidly losing stationary phase, entrained by the mobile phase as a low concentration suspension of minuscule droplets, which provided irreproducible analyses. The need to saturate the mobile phase with the organic compounds used as the stationary phase caused major detection problems. The use of liquid stationary phases was abandoned.

The development of purer brands of porous silica, of chemically bonded silica, and the use of more appropriate solvent mixtures permitted the replacement of LLC with liquid–solid chromatography (LSC). Superficially porous packing materials were found to have low loading capacity in LSC while finer and finer fully porous particles were produced, permitting the production of more efficient columns and nullifying the potential advantages of the existing controlled-porosity particles. This marked the end of the first generation of this type of particles.

3.3.1. The origins of Zipax, the controlled surface porosity particles

Convinced that the availability of better particles would markedly improve the performance of liquid chromatography, Kirkland in cooperation with Iler [61], designed, prepared, and manufactured a new brand of highly performing particles, which were named “controlled surface porosity” particles or CSP [10,62]. This material was later described as made by coating successive monolayers, each 200 nm thick, of a silica sol onto 55 μm glass beads, producing a porous crust that could later be impregnated with a stationary liquid phase. Fig. 4 shows SEM of several particles, of a cross-section of a particle and of its surface. As shown by Fig. 4b, the shell thickness was approximately 2 μm. This suggests that the finally commercialized product was not the one initially studied.

Kirkland described the properties and some applications of Zipax shortly after the initial work of Horváth and Lipsky [10,63]. The concept of CSP particles was most attractive in the years when HPLC began to attract great interest. At that time, the samples of porous silica that were produced had a markedly acidic surface, due to the presence of relatively large concentrations of Lewis acids on their surface, particularly boron and iron ions. The peaks of even moderately polar compounds eluted from columns packed with porous silica particles exhibited significant tailing. Analysts thought that better results would be obtained with packing materials similar to those successfully used in gas chromatography, made of porous particles having a large porosity but a low specific surface area, coated with large amounts of a fluid organic substance. Chromatography would be based on liquid–liquid equilibria. The silica particles should merely be the support of this liquid. This was why particles like Zipax, which had a low porosity and a low specific surface area were attractive. As explained earlier, the first generation of CSP particles was short-lived.

3.3.2. Preparation and properties of Zipax

The commercialized Zipax was made of a solid silica core surrounded by five thick layers of 200 nm silica spheres [64]. The specific surface area of these layers was 15 m^2/g and the aver-

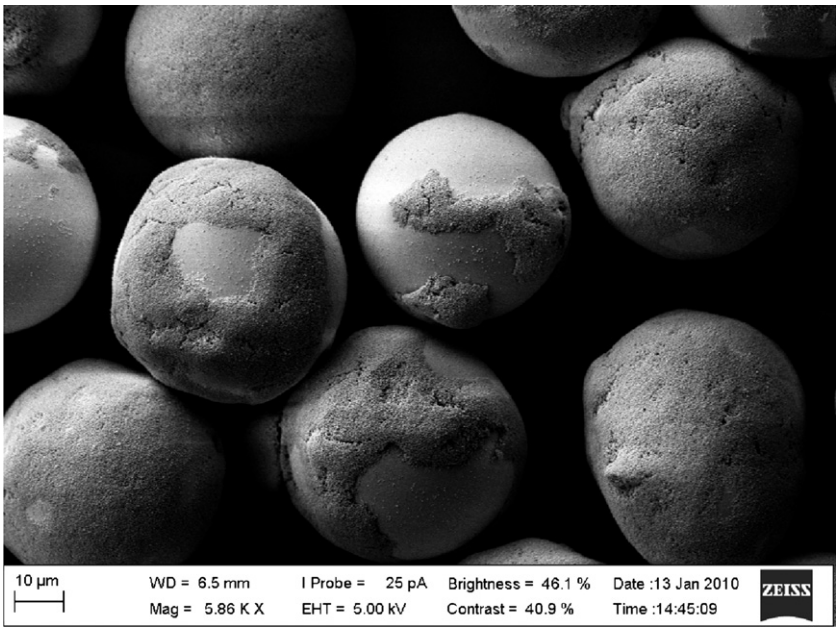

Fig. 4. SEM of a CSP sample recovered from storage after 40 years; it illustrates the structure of the layer.

age pore size 1000 Å. Although competition rapidly offered similar products, Zipax seems to have been the product that exhibited the best level of performance of this type of packing materials. It was certainly the most studied and remains the best documented CSP material of this period [10,17,18,63,64].

Done et al. [18] packed 2 mm × 1000 mm long columns with Zipax, Corasil and Porasil particles. The Zipax product was sieved into four different fractions, which gave nearly the same reduced HETP plots (see Fig. 5). The particles were coated with 2% of β,β'-dipropionitrile. The reduced HETP plots (see Fig. 5) show performance comparable to those of excellent modern columns, with h_{min} between 1.80 and 2.0 and u_{opt} around 4.5 [17]. These plots show also a significant decrease of the column efficiency with increasing retention factor (see Fig. 5). Yet, the minimum reduced HETP still hovers around 2 and the C term is 0.011 at $k' = 7.8$, which is excellent by present standards. This suggests that the classical assumption that lingers in HPLC for nearly 40 years, that *good chromatographic performance requires high uniformity of particle size* [18] have little validity. The only serious problem encountered in using batches of particles with a wide range of diameters is in the selection of the most suitable diameter to use when calculating the reduced plate heights and velocities. Unfortunately, the actual HETPs of the Zipax columns were poor because, due to the large particle size, they had to be operated at relatively high mobile phase velocities, corresponding to reduced velocities of several hundred for small molecules, giving HETPs of the order of 4.5, a value consistent with the chromatograms published ($t_0 \simeq 1$ min, $u_0 \simeq 17$ cm/s, $\nu \simeq 500$, $N \simeq 4000$, $H \simeq 250$ µm, with the results of Kennedy and Knox [64] and the earlier results of Kirkland [63]. This last work is mostly devoted to the development of suitable packing methods for the raw Zipax material, which had a much wider particle size distribution than the narrow cuts used by Done et al. [18] and, consequently, provided lesser efficiencies.

As indicated by Kennedy and Knox [64], Zipax cannot be used in the now classical LSC mode, the surface area of the column being too small. Yet, the efficiency data for non-retained compounds are in excellent agreement with those shown in the top panel of Fig. 5. The A coefficient of the Knox equation is smaller for the Zipax than for the Corasil columns and for fully porous particles [64]. This was the first observation that CSP particles made with multiple layers of silica particles seem to pack markedly better than conventional fully porous particles. Also, this coefficient seemed to depend on the retention factor [64], as will be demonstrated later [65]. It is noteworthy that a 4.6 mm × 300 mm column packed with a sample of Zipax (see Fig. 4, average d_p = 55 µm) recovered earlier this year from an Agilent warehouse gave a minimum reduced HETP of 2.05 at a reduced velocity of ca. 3.5 for naphtho[2,3,a]pyrene ($k' = 0$), eluted with acetonitrile (data not shown).

In the 1970s, chemists found and developed reactions allowing the bonding of chemical groups to the surface of silica and the preparation of chemically bonded porous silica particles that were highly stable within a sufficiently wide range of experimental conditions. At the same time, the preparation of smaller particles developed progressively. The need of packing materials suitable for liquid–liquid chromatography disappeared.

3.3.3. Applications of Zipax

Before it became known and commercialized as Zipax, this material was prepared, used and studied by Kirkland as controlled surface porosity support [9,66]. It became later the support for Permaphases. To avoid the difficulties encountered later by the proponents of LLC, Kirkland coated the thin shell of the particles with a layer of a polymer or cross-linked polymer that was insoluble in the mobile phase [9].

Besides its use as a support for the stationary phase in LLC, Zipax was used as a support for ion exchangers [9,66]. Kirkland used columns packed with Zipax particles coated with either a thin layer of cation exchanger, a fluoropolymer containing strong sulfonic acid moieties or a thin layer of an anion exchanger containing strongly basic tetraalkylammonium groups [66]. The exchange capacities of the cation exchange column was 3.5 µeq/g and that of the ion exchanger was 12 µeq/g. The columns exhibited excellent long time stability (months). They were used to analyze nucleotides and nucleic acid bases. The complete separation of the four bases was achieved in 5 min at 63 °C, with a flow rate of 2.0 ml/min of a 0.01 N nitric acid, on a 2.1 mm × 1000 mm column. The separation of other purines and pyrimidines could also be performed by adjusting the buffer composition. An increase in the temperature improved the column efficiency. Rapid separations of ribonucleoside-5′-monophosphoric acids were made on

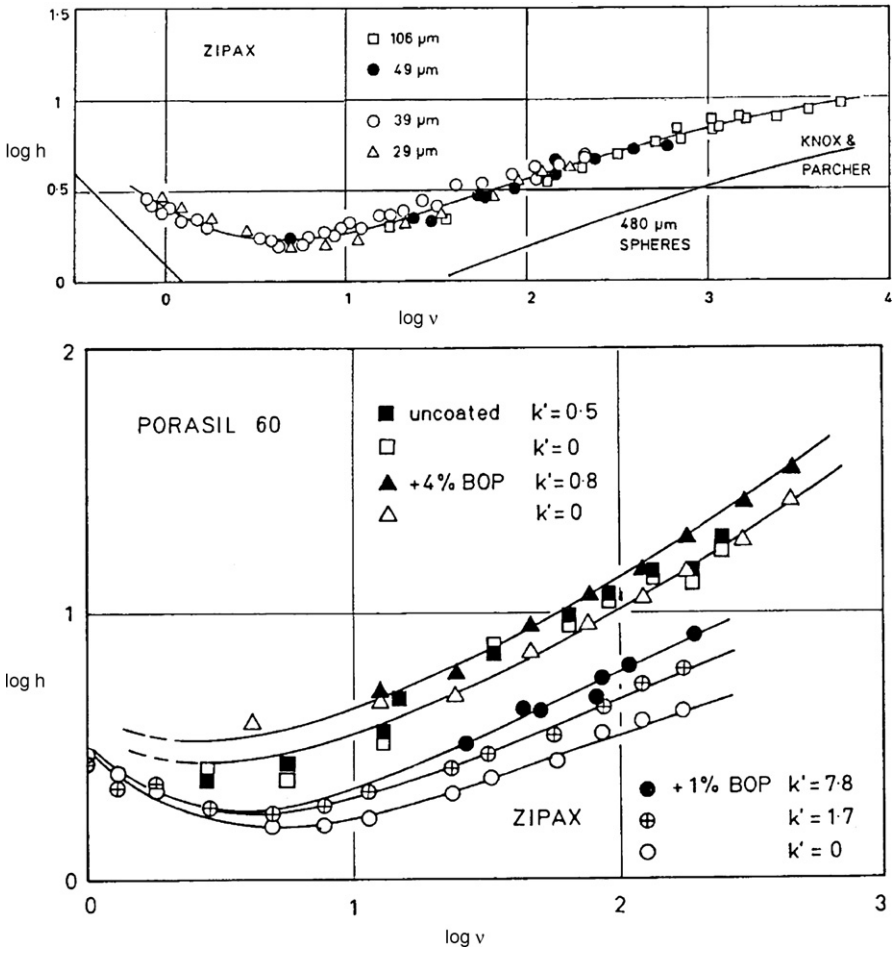

Fig. 5. Top: reduced HETP of columns packed with four fractions of Zipax, for cyclohexane eluted with chlorobenzene at room temperature ($k' = 0.0$). Reproduced from [64], Fig. 2. Bottom: reduced HETP of a Zipax and a Porasil column. Reproduced from [18], Fig. 2.

the anion exchanger column. The separation of 5′-CMP, 5′-UMP, 5′-AMP, and 5′-GMP was achieved in 6 min. Mixtures of the 2′- and 3′-ribonucleosides were separated under similar conditions.

3.3.4. Preparation and properties of Permaphases

When it had been established that the LLC columns were not sufficiently stable and that alkyl-bonded porous silica were performing much better separations, it became clear that the specific surface area of Zipax was too small and that the retention volumes of analytes on a chemically bonded monolayer would be insufficient to provide useful separations. In an attempt to solve this problem, Kirkland [67] developed in the early 1970s a method of synthesis of pre-polymerized tri-functional silanes, which were then bonded to the silica surface inside the porous crust of Zipax particles, forming on this support a layer of polymer amounting to ca. 1% by weight of the packing material [67,68]. This product was marketed as Permaphases ETH (with a polyether layer) and ODS (with a polymeric octadecyl polysiloxane).

The performance of this packing material was discussed by Kirkland [67], Schmidt et al. [69], Beachell and DeStefano [70], and Knox and Vasvari [71]. The efficiencies obtained with columns packed with either Permaphase ETH or ODS were lower than those

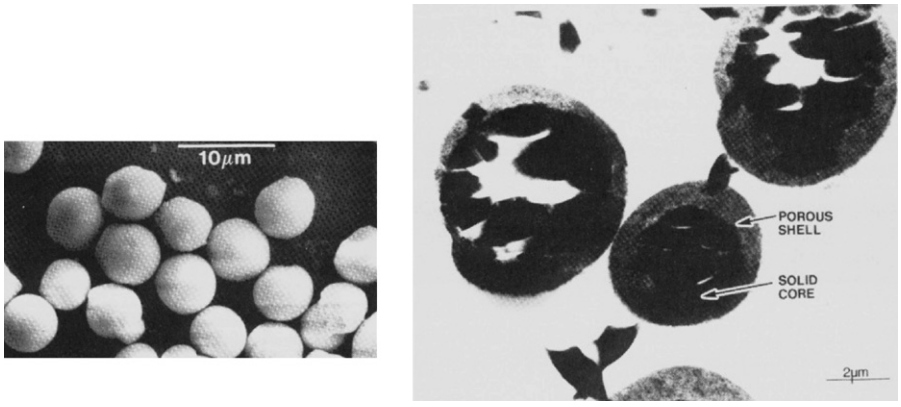

Fig. 6. Scanning electron micrograph of the early Poroshell particles (top) and transmission electron micrograph of these particles cross-sections [16].

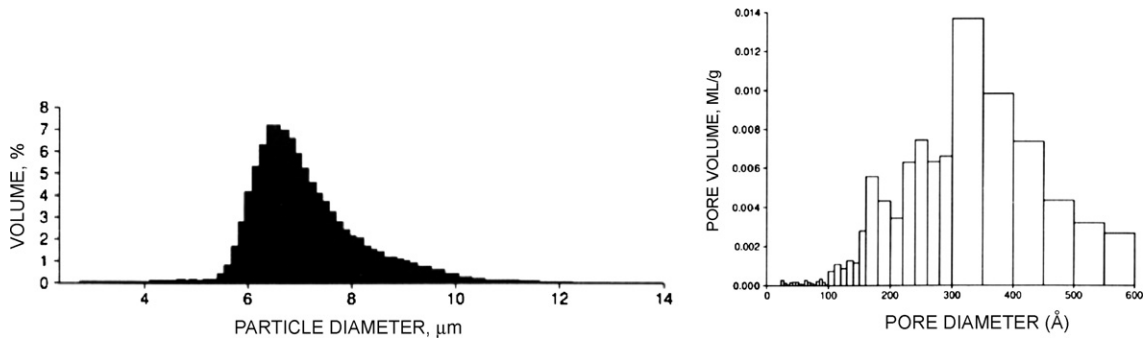

Fig. 7. Particle size distribution of the early Poroshell particles (top) and BET pore size distribution of these particles (right) [16].

obtained with Zipax, suggesting that slow diffusion in the polymer layer resulted in slow mass transfer kinetics and in the large value found for the *C* coefficient of the van Deemter plot. This suggestion was confirmed by the lack of dependence of the reduced HETP on the temperature [71]. It seems, however, that retention factors on Permaphase ODS and the degree of symmetry of the eluted peaks depended significantly on the sample size, in contrast with Permaphase ETH, for which these peak parameters were constant [71]. Because the degree of peak asymmetry was alleviated when the mobile phase velocity was increased, the explanation proposed then seems now doubtful.

3.3.5. Corasil

Corasil was a packing material made of pellicular particles manufactured by Waters in the 1970s, for the same purpose as was Zipax, as a support for a stationary liquid phase. It was made by coating a layer of ground-up silicagel on glass beads, to create a porous adsorbent layer. There were two brands, Corasil I and II, made of solid glass spheres surrounded by layers of this silicagel, 7 and 14 m^2/g for Corasil I and II, respectively. The average pore size of these layers was ca. 50 Å; the average particle size was between 44 and 53 μm [64]. As Zipax, Corasil was used in the LLC mode, with a small amount (ca. 1%) of β, β'-dipropionitrile impregnating the layer of porous silica. The reduced HETP curves reported by Kennedy and Knox [64] are similar to those that they also reported for Zipax, the main differences being that no data point were measured at reduced velocities lower than ca. 20 and that the efficiency of the Corasil columns decreased more rapidly with increasing retention factors. The column efficiencies of the columns packed with the two Corasil materials are nearly identical.

3.4. The second generation of core–shell particles

A second generation of core–shell particles appeared in 1992, with the development of 5 μm Poroshell 300 (Agilent) [16]. In this initial report, the particles were 7 μm in diameter and had a 1 μm shell thickness. The particles were made by spray-drying a suspension of the core particles, solid silica beads in an aqueous silica sol. The cores were made by sintering narrow-pore Zorbax particles at 1050 °C for 4 h, which reduces their specific surface area to less than 1 m^2/g. A 5 μm size fraction was isolated by elutriation and coated with a single layer of colloidal silica to ensure adhesion of the spray-dried coating. The average size of the silica sol particles was 44 nm. The pH of the solution was adjusted to 9 with dilute ammonium hydroxide. Nearly uniform porous shells formed around the cores. Heating the particles in air at 540 °C to eliminate residual organics and then sintering them at 1000 °C for 2 h strengthened them. This procedure gave porous shells with a 0.5 μm thickness, so a second layer was added, using the same procedure. This was followed with rehydroxylation of the porous silica and surface modification, which provided the final material, which was easily packed [16]. Fig. 6 shows micrographs of the first Poroshell particles in SEM and transmission. Comparison of these micrographs with those showing Zipax (see Fig. 4) and Halo (see later, Fig. 9) illustrates the dramatic improvements made over 40 years in the methods of producing core–shell particles.

The particle size distribution of the initial Poroshell packing material (see Fig. 7) was narrower than that of conventional fully porous particles and unsymmetrical, with 80% of the particles between 6.1 and 8.5 μm. The pore distribution was also wide, between ca. 100 and 600 Å with a maximum at 300–350 Å (see Fig. 7). The internal pore volume was sufficient to permit SEC separations of polystyrene standards in the range between 2000 and 200,000 Da; the specific surface area was large enough to allow the use of samples of significant size without column overloading. The column efficiency for polystyrene samples decreased much less with increasing molecular weight than that of fully porous particles made with the same silica, supporting the assumption that pore diffusion is faster in core–shell particles than in fully porous ones, but the minimum value of the HETP achieved was disappointing, with a minimum reduced value around 7 [16]. Due to the low phase ratio of columns packed with core–shell particles, the retention of analytes on these columns is lower than their retention on columns packed with fully porous particles, so their elution requires lower concentrations of organic modifiers.

The columns packed with Poroshell 300 have met only with limited success, in spite of allowing excellent separations of peptides in gradient elution [72,73]. The efficiency of a commercial Poroshell 300SB (Agilent) was found to be better than that of a comparable Zorbax column. This improvement was due to the slightly lesser values of the *A* and *C* coefficients of the best plate height equation and to an almost half smaller *B* coefficient, due to the lesser internal porosity. This translated into minimum values of 2.6 for the former and 3.2 for the latter [72], showing a significant but moderate improvement. In a systematic comparison, Urban et al. [74] found that the Poroshell 300 column performed better for the separation of proteins than columns packed with fully porous particles. It seems that the actual performance of the Poroshell columns was markedly improved between their initial development and their commercialization.

4. The modern core–shell particles or the third generation

Real success of the core–shell particle concept came in 2006, with the introduction of the 2.7 μm Halo core–shell particles of Advanced Material Technologies [31,59,75]. The exceptional properties of the Halo columns impressed the whole community and considerable attention was paid to them. The drawback of the low loading capacity of the initial core–shell particles was mostly eliminated in the modern ones by building a 0.5 μm thick porous shell around a 1.7 μm core. Thus, the shell occupies about 75% of the volume of the 2.7 μm particle. The most striking result was the

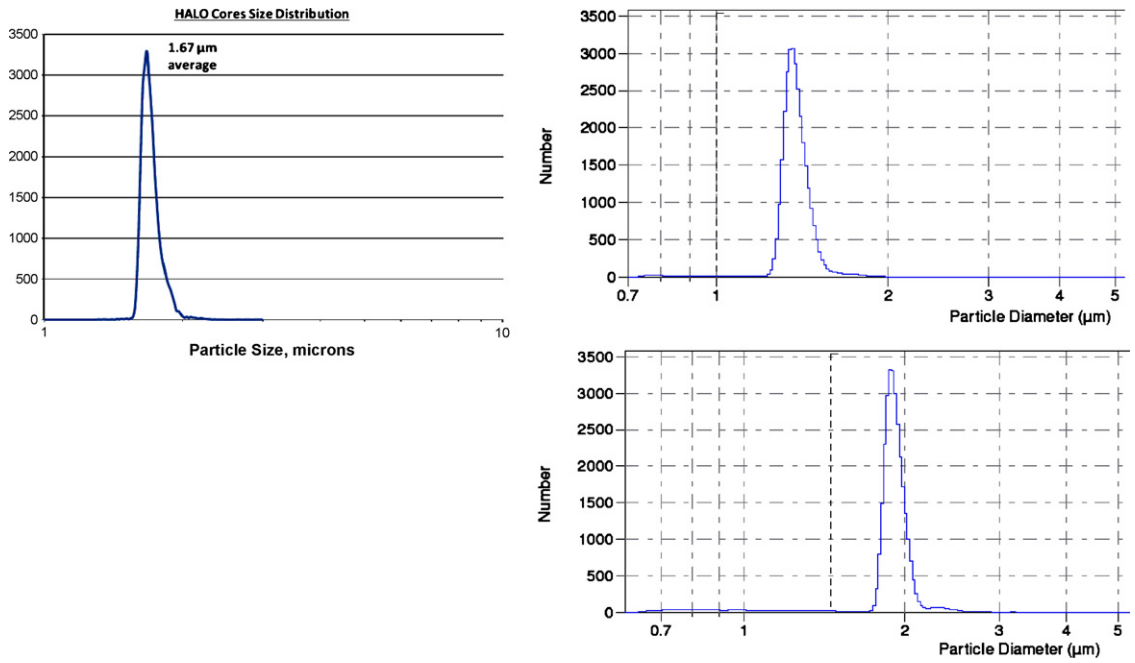

Fig. 8. Size distribution (Coulter counter technique) of top left: the 1.7 μm non-porous silica Halo cores used to prepare the 2.7 μm Halo core–shell particles; top right: the 1.2 μm non-porous silica Kinetex cores used to prepare the 1.7 μm Kinetex core–shell particles; bottom right: the 1.9 μm non-porous silica Kinetex cores used to prepare the 2.6 μm Kinetex core–shell particles.

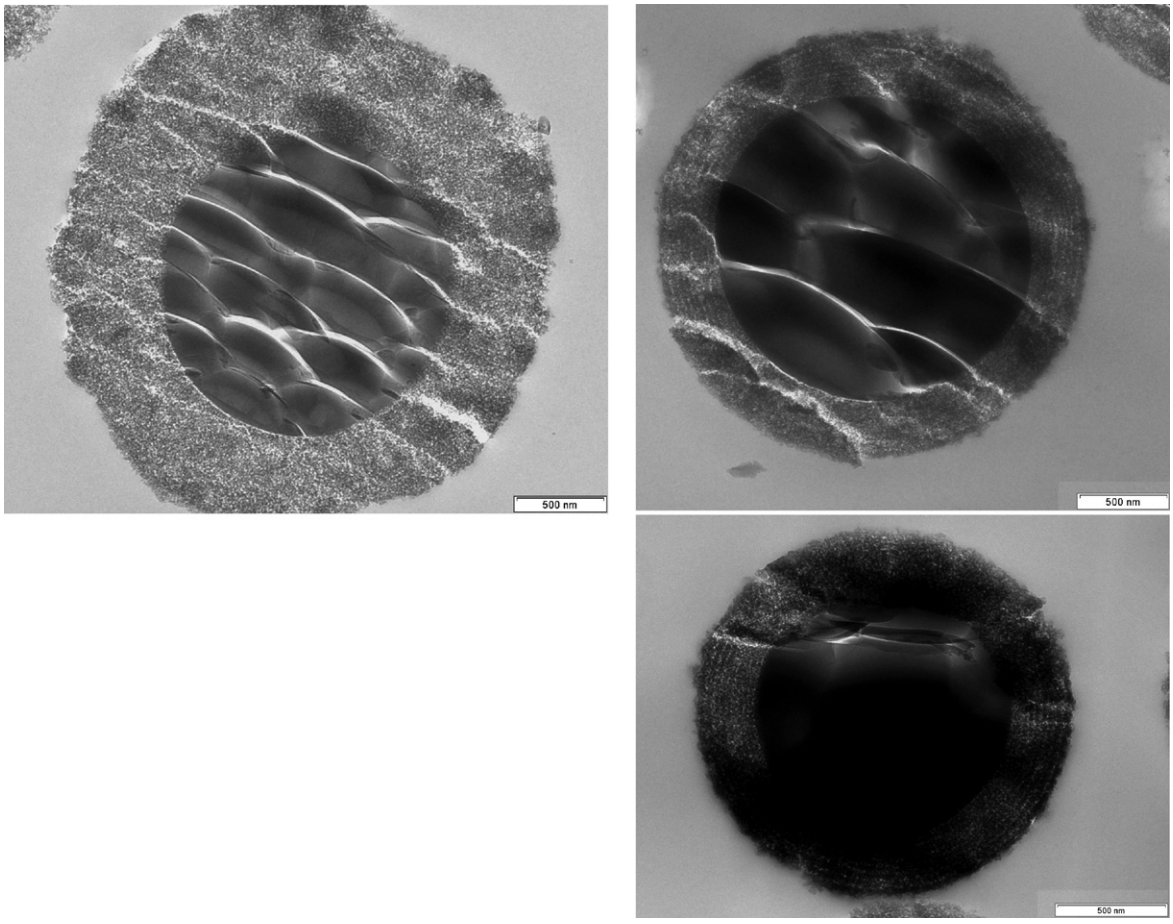

Fig. 9. SEM cut of top left: a 2.7 μm Halo core–shell particles; top right: a 2.6 μm Kinetex core–shell particles. Note the layer stratification of the porous shell revealing the step-by-step growing process of the porous shell; bottom right: a 1.7 μm Kinetex core–shell particles. Note, as in the top right figure, the layer stratification of the porous shell revealing the step-by-step growing process of the porous shell.

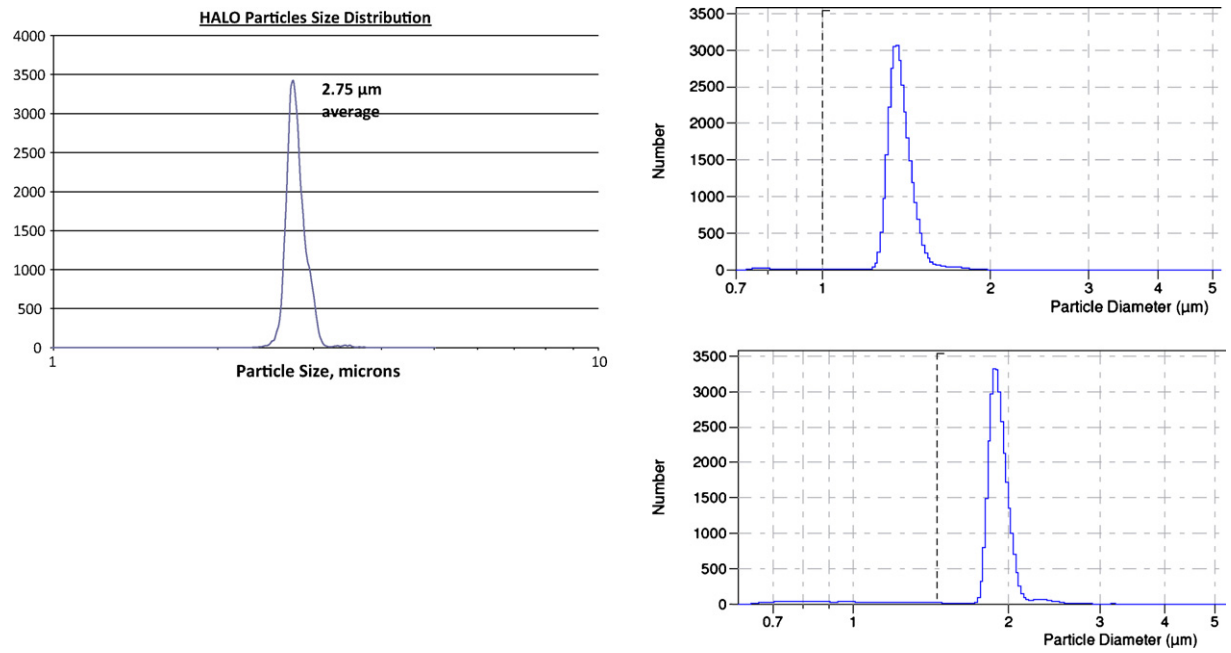

Fig. 10. Size distribution (Coulter counter technique) of top left: the 2.7 μm Halo core–shell particles; top right: the 1.7 μm Kinetex core–shell particles; bottom right: the 1.7 μm Kinetex core–shell particles. Note that the variances of these distributions are the same as those of the distributions shown in Fig. 8 for these cores.

early achievement of 4.6 mm I.D. columns with a minimum reduced plate height of 1.5 for small molecules [76]. This new packing material was designed for the separation of small molecular weight compounds [32]. Three years later, Phenomenex offered columns packed with the 2.6 then the 1.7 μm Kinetex particles which exhibit exceptional performance, with a small h_{min} = 1.2 [37,77], a small C term [32,78], and a very flat HETP curve for medium-size molecules. Earlier this year, Agilent came up with the new 2.7 μm Poroshell 120 while Advanced Material Technologies launched a second brand, the 2.7 μm Halo-ES-peptide core–shell particles [79] providing exceptional performance for peptides and small proteins [79]. Packed in 4.6 mm I.D. tubes, all these particles give columns exhibiting plate heights equivalent to those achieved with the latest state-of-the-art sub-2 μm particles, with H between 3 and 4 μm.

4.1. Preparation and properties of the modern core–shell particles

4.1.1. Preparation of the modern core–shell particles

The starting material (also called starting seed) for the preparation of modern core–shell particles are typically sub-2 μm and sub-3 μm nonporous spherical silica particles. They are prepared *via* a controlled growth process [80] which produces non-porous silica particles (<2 μm) with very narrow particle size distributions after modification of the well-known Stober protocol [81]. The Stober process provides nearly monodisperse non-porous silica particles. Fig. 8 shows the PSDs of the nonporous silica cores used to fabricate the 2.7 μm Halo particles, the 1.7 μm Kinetex core–shell particles, and the 2.6 μm Kinetex core–shell particles. The ratios $d_{90\%}/d_{10\%}$ of these size distributions lie between 1.11 and 1.14. In comparison, the same ratio with fully porous particles is usually between 1.3 and 2.0.

The main challenge in the preparation of core–shell particles is to build a stable and homogeneously thick layer of porous shell around the solid cores. A very popular synthesis route consists in using template surfactants for ordered mesoporous silica [82,83]. Such standard methods only deliver thin shells (≃60 nm) with very small average pore sizes (≃30 Å), which makes the particles incompatible with their packing in columns for liquid chromatography. Thick shells with large mesoporous volume is demanded for use in liquid chromatography. They can be made in the presence of both a charged adsorbing surfactant, cetyltrimethylammonium bromide (C_{18}TABr), and an organic expander such as polyethyleneglycol-polypropyleneglycol-polyethyleneglycol block co-polymer [84]. Shells with thicknesses of 150–350 nm can then be prepared. Fig. 9 shows SEM photographs of the cuts of core–shell particles (2.7 μm Halo, 1.7 μm Kinetex, and 2.6 μm Kinetex). The average thickness of these shells are 600, 270, and 350 nm, respectively.

It is important to mention that really thick porous shells cannot be obtained in a single synthesis step. Several successive steps are made, following the same route: the growth seeded nonporous silica particles are suspended in a mixture of ethanol and water. A solution mixture of the ionic, organic surfactant (C_{18}TABr and of the pore expander polymer) is prepared in the same mixture of ethanol and water. A highly concentrated solution of ammonium hydroxide is poured into the silica dispersion. Silanols groups are then negatively charged at the surface of the non-porous particles. The surfactant solution is added to the silica dispersion and is allowed to equilibrate at a fixed temperature at atmospheric pressure. The positively charged surfactant, $C_{18}TA^+$, is adsorbed to the silica particle in the presence of the organic polymer. Then, pure tetraethyl orthosilicate (TEOS) is added to the suspension in order to build the porous structure of silica around the adsorbed surfactant molecules. Finally, the new formed particles are centrifuged and then serve as the starting seed silica particles in the next step. The same process is repeated until the desired shell thickness is reached.

Pore expansion is achieved by preparing a solution of N,N-dimethylhexadecylamine (DMHA), C_{18}TABr, and trimethylbenzene. This solution is used as a dispersant for the synthesized silica core–shell particles and is heated during a three days period. Finally, the surfactant is removed by calcination at high temperature. In Fig. 9, the empty spaces left after calcination allow to identify the repetition of the step process. A multi-layer silica structure is clearly visible in these SEM photographs.

The above description of the fabrication process of the core–shell particles is very general, although the details certainly differ from one manufacturer to the next (Advanced Material Technology, Phenomenex, and Agilent Technologies) regarding the nature of the chemicals used, their concentration, the temperature

applied, and the reaction times. Overall, however, the general principle based on using a surfactant template agent and repeating the synthesis of a silica monolayer remains the same.

4.1.2. Physico-chemical properties of the modern core–shell particles

The precise control of the thickness of the porous shells allows the preparation of core–shell particles with a narrow size distribution, which is nearly the same as the size distribution of the starting nonporous silica seed around 1.11–1.13 [32]. Fig. 10 shows the size distributions of the 2.7 μm Halo, 1.7 μm Kinetex, and 2.6 μm Kinetex particles. The $d_{90\%}/d_{10\%}$ ratios of the corresponding silica cores provided by the Coulter counter technique were 1.122, 1.115, and 1.126. For the core–shell particles, they are 1.112, 1.118, and 1.128, respectively. Some authors claim that this physico-chemical property is important for the preparation of highly homogeneous chromatographic beds, hence of highly efficient columns [85]. However, this is arguable. Calculations show that the gain in reduced plate height is of the order of 0.1 h unit [86] when the RSD of the particle size distribution decreases from about 15% (1.7 μm BEH fully porous particles) to 5% (2.6 μm Kinetex core–shell particles).

Another important property of core–shell particles is the volume fraction occupied by the shell. A sufficiently thick porous shell should be prepared in order to achieve a reasonable sample capacity. Too small a specific surface area, too small would be the retention factor. As a result, the concentration of the strong eluent in the mobile phase needs to be decreased. Therefore, the adsorption energy may increase strongly and peak tailing caused by thermodynamic overloading of the most active adsorption sites could become signifdicant [87–90]. The Coulter counter method data provide measured volume fractions occupied by the porous shell in 2.7 μm Halo, 1.7 μm Kinetex, and 2.6 μm Kinetex particles that are equal to 80, 63, and 58%, respectively. Based on the shell thickness claimed by the manufacturer of the 2.7 Poroshell120 particles, the same volume fraction in this last brand of core–shell particle is estimated at 75%. In conclusion, these modern core–shell particles can provide between 60 and 80% of the specific surface area of the same but fully porous particles. Unless the specific surface area of the porous shell happens to be unusually low, e.g., lower than 50 m^2 per gram of porous silica (the mass of the silica core being excluded), these modern core–shell particles will not require the use of weak eluent mixture.

The specific surface area of these materials was first measured by low temperature nitrogen adsorption [32], providing values of 124, 98, and 100 m^2/g with the 2.7 μm Halo, 1.7 μm Kinetex, and 2.6 μm Kinetex silica particles. Note that these values refer to the unit mass of whole particles, including the nonporous core and the shell. When corrected per unit mass of porous silica (shell only), they increase to 237, 243, and 319 m^2/g, respectively. Taking into account the volume fraction of the shell in these particles, they are equivalent to fully porous particles having specific surface areas of 190, 153, and 185 m^2/g. Obviously, the chemical modification of the surface of silica by grafting long C_{18} alkyl chains affects the pore volume [91–94]. Unfortunately, the LTNA technique does not apply straightforwardly with silica-C_{18} surface because the specific surface occupied by an adsorbate molecule of nitrogen on this hydrophobic surface is unknown. Yet, assuming that the average length of the bonded C_{18} chain is of the order of 7 Å [95], Fig. 11 shows the expected shift of the pore size distribution of these three porous shells. The estimates of the corrected surface areas are 124, 158, and 211 m^2/g, standard values for fully porous particles. In conclusion, sample overloading is not an issue with this new generation of core–shell particles.

The average mesopore size and its distribution is a crucial structural parameter, particularly when the analysis of large molecules

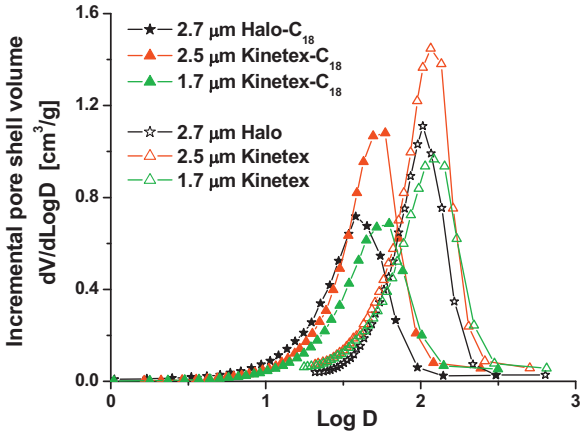

Fig. 11. Pore size distributions of the porous shells of the 2.7 μm Halo 90 Å, 2.6 μm, and 1.7 μm Kinetex 100 Å core–shell particles before (empty symbols) and after (full symbols) C_{18} derivatization of the surface area. All pore volumes refer to 1 g of porous silica. Note that Kinetex has a wider distribution than Halo.

such as proteins is concerned. Because their molecular sizes are large, proteins can be significantly excluded from the mesopore network of the particle, leading to a poor retention and to distorted peak shapes [79]. Fig. 12 shows the plots of the pore size distributions of 2.7 μm Halo, 1.7 μm Kinetex, and 2.6 μm Kinetex particles.

The average mesopore sizes of current core–shell particles are typically around 100 Å, demonstrating the success of the synthesis and pore enlargement processes described above. It was shown that larger mesopores are generated in the Kinetex than in the Halo core–shell. As a result, it was estimated that the accessible volumes of these shell to insulin were 13 and 4% for Kinetex and Halo particles, respectively. The limited access to the internal pore volume of the Halo core–shell explains the poor efficiency of the Halo column for large proteins [79,96].

Finally, another interesting property of core–shell particles is the enhanced roughness of their surface compared to that of fully porous particles. Fig. 13 compares the SEM photographs of one single fully porous particle (3 μm Luna) and that of one single core–shell particle (2.7 μm Halo).

The difference in the external surface roughness reflects the specific preparation technique of these two types of particles (sol–gel process for the former, coarcevate colloidal particles or step-by-step templating agent process around a non-porous solid core for the latter). It is not surprising that the step-by-step superposition

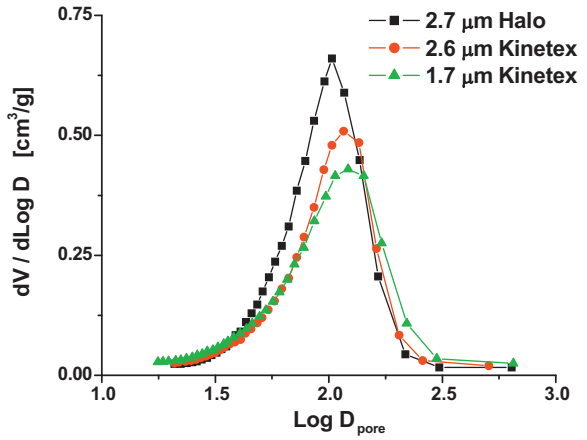

Fig. 12. Pore size distributions of the 2.7 μm Halo 90 Å, 2.6 μm, and 1.7 μm Kinetex 100 Å silica core–shell particles. The pore volumes refer to 1 g of packing material, including the mass of the solid silica core.

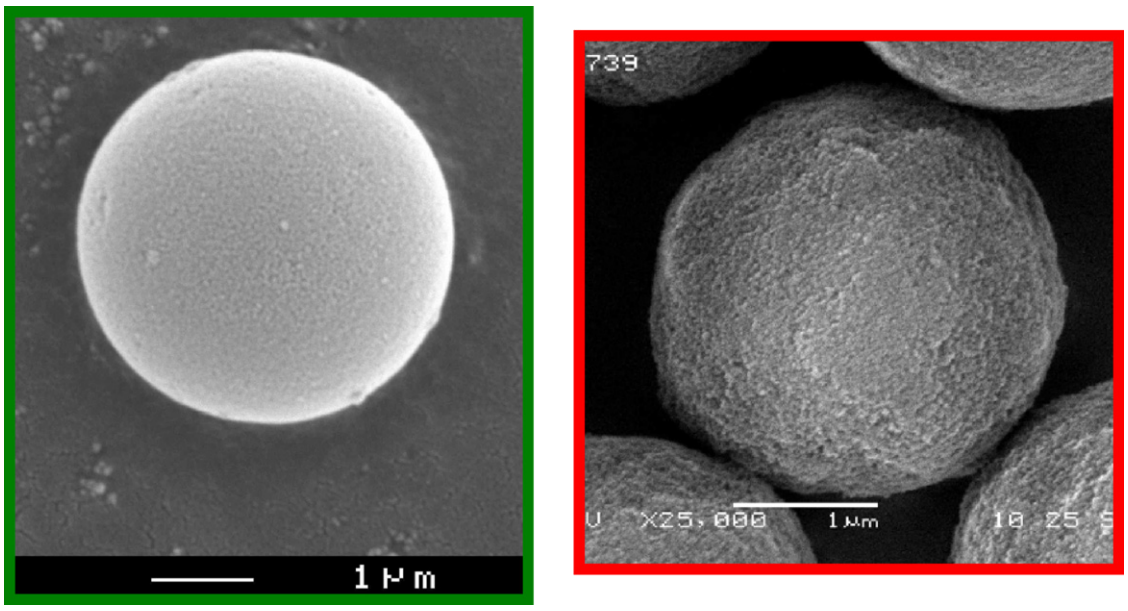

Fig. 13. SEM zoom in to a single fully porous 3 µm Luna (left) and core–shell 2.7 µm Halo (right) particles . Note the difference in the roughness of the external surface area.

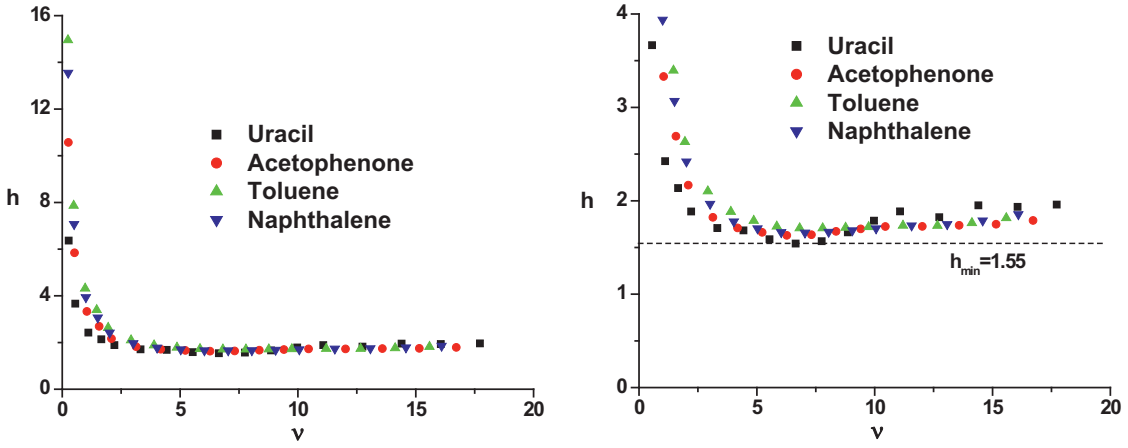

Fig. 14. Plot of the reduced HETP of four small molecules versus the reduced interstitial velocity. Left: HETP measured on a 4.6 mm × 150 mm column packed with 2.7 µm Halo-C_{18} core–shell particles; right: same as in left figure but the plot is zoomed into the minimum range of the HETP plot. Note the minimum reduced plate height of 1.55 and the flat *C* term.

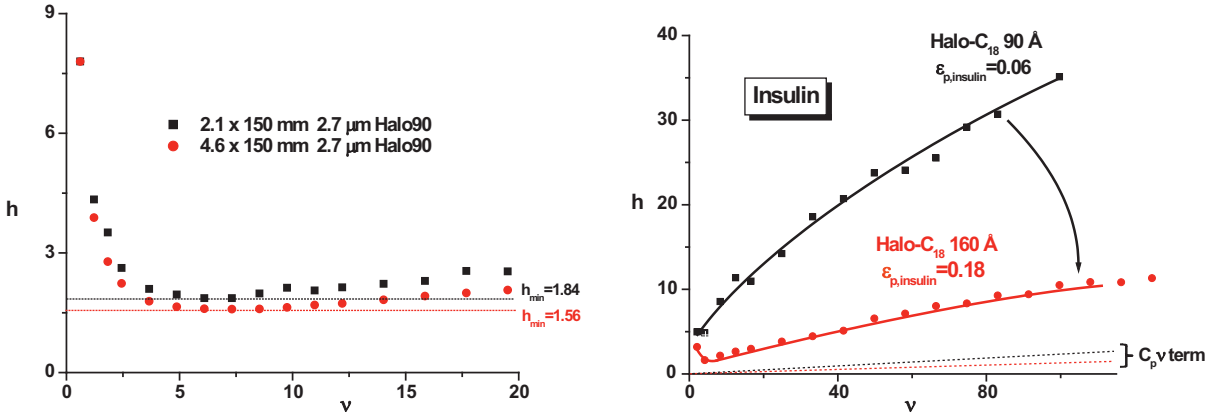

Fig. 15. Left: comparison between the reduced HETP of naphthalene measured with a 4.6 mm × 150 mm and a 2.1 mm × 150 mm columns packed with the same 2.7 µm Halo-C_{18} packing material. The actual mobile phase flow rate and velocity corresponding to $\nu = 10$ are 1.5 ml/min and 0.38 cm/s, respectively. Right: comparison between the plots of the reduced HETP of insulin versus its reduced interstitial velocity on a 4.6 mm × 150 mm column packed with 2.7 µm Halo-C_{18} core–shell particles with two different average mesopore sizes. The actual mobile phase flow rate and velocity corresponding to $\nu = 10$ are 0.225 ml/min and 0.06 cm/s, respectively.

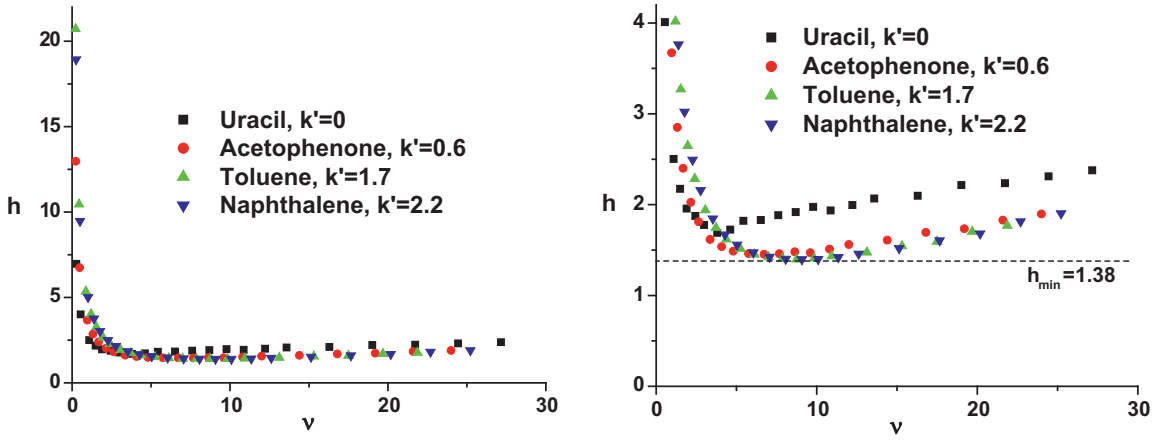

Fig. 16. Plot of the reduced HETP of four small molecules versus the reduced interstitial velocity. Left: HETP measured on a 4.6 mm × 150 mm column packed with 2.6 μm Kinetex-C_{18} core–shell particles; right: same as in left figure but the plot is zoomed into the minimum range of the HETP plot. Note the minimum reduced plate height of 1.38 and the flat *C* term.

of porous silica monolayers around a template agent generates a rather rough external surface after accumulation of about ten silica monolayers. The roughness of the particles may play an important role during the slurry packing process of these particles. It may contribute to increase the shear stress between these particles, to reduce the differential radial strain, from the center to the wall of the column tube, and therefore, to reduce the differential interstitial linear velocity between the center and the wall of the column. This likely contributes to minimize the trans-column eddy diffusion term in the general van Deemter equation.

4.1.3. Chromatographic properties of modern core–shell particles

The chromatographic properties of modern core–shell particles were first reported with 4.6 mm I.D. columns. The reduced HETPs of 2.7 μm Halo, 2.7 μm Halo-ES-peptide, 2.6 μm Kinetex, and 2.7 μm Poroshell120 were reported recently [37,78,79,96,97]. We now summarize the characteristics of these columns in terms of their reduced plate heights for small molecules (reduced interstitial linear velocity $\nu < 30$) and for large proteins (insulin and/or lyzozyme, $\nu < 100$). It is important to report here that the external porosity of columns packed with sub-3 μm core–shell particles is systematically larger than that usually observed with columns packed with fully porous particles, which confirms that stress and strain distributions are different in columns packed with these two types of particles, as explained above. The average value of ϵ_e is typically 0.40 with silica-C_{18} core–shell particles [32] while it is around 0.37 with conventional silica-C_{18} particles. This difference in external porosity underlines the larger difficulty found when trying to densely pack rough spherical particles than when packing smooth spherical ones.

All the HETPs reported and analyzed below were measured using the moments of the elution bands.

- Kinetic properties of Halo columns

  Fig. 14 (left) shows plots of the reduced plate heights of four small molecules (uracil, acetophenone, toluene, and naphthalene) for a 150 mm × 4.6 mm I.D. column packed with 2.7 μm Halo-C_{18} particles, with an average mesopore size of 90 Å, which was the first generation of sub-3 μm core–shell particles. The temperature was set at room temperature; the eluent was a mixture of acetonitrile and water (80/20, v/v). Fig. 14 (right) zooms onto the lower part of this graph and locates precisely the minimum reduced HETP, which is equal to 1.55. The C-branch remains nearly flat up to reduced linear velocities close to 20. The minimum reduced plate height is nearly the same for all four compounds, which suggests that the trans-column eddy diffusion term is extremely small in this column, otherwise the reduced plate height would be significantly smaller for the more retained compound, naphthalene [98]. This observation was confirmed by local electrochemical detection of the elution profile across the outlet of the 4.6 mm I.D. column which showed a relative velocity bias of only 0.3% [32,99].

  Fig. 15 (left) shows that the minimum reduced HETP of naphthalene for a 2.1 mm I.D. column packed with the same material is slightly larger (1.84 versus 1.56) than for the standard 4.6 mm I.D. columns. Recent investigations demonstrated that the origin for this difference is the larger radial distance over which velocity gradients are established in narrower bore columns.

  The manufacturer of columns packed with Halo-C_{18} 90 Å core–shell particles warned that these columns are not suitable for the analysis and separation of large molecules, with molecular weights exceeding 5 kDa. This is why the company recently released the second generation of Halo particles, the 2.7 μm Halo-ES-peptide, which was designed to provide better efficiency for large molecules. Fig. 15 (right) confirms that the C-branch of this column is flatter with the second than with the first generation of Halo core–shell particles. A deeper investigation, involving the measurement of the trans-particle mass transfer resistance coef-

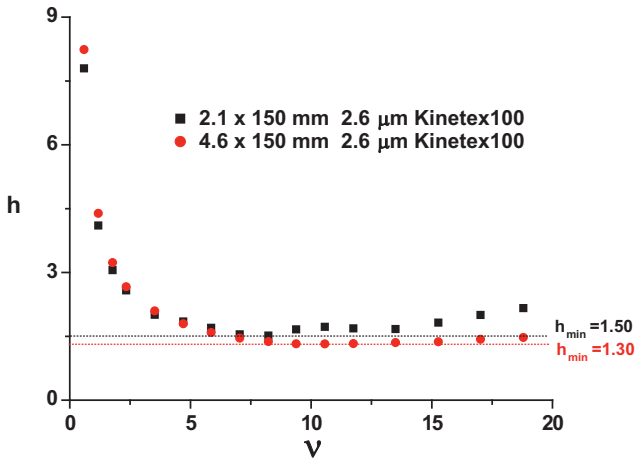

Fig. 17. Effect of the column inner diameter on the plot of the reduced HETP of naphthalene on a 4.6 mm × 150 mm and a 2.1 mm × 150 mm column packed with 2.6 μm Kinetex-C_{18} core–shell particles. Note the better performance of the large I.D. column at high flow rates. The actual mobile phase flow rate and velocity corresponding to $\nu = 10$ are 1.5 ml/min and 0.38 cm/s, respectively.

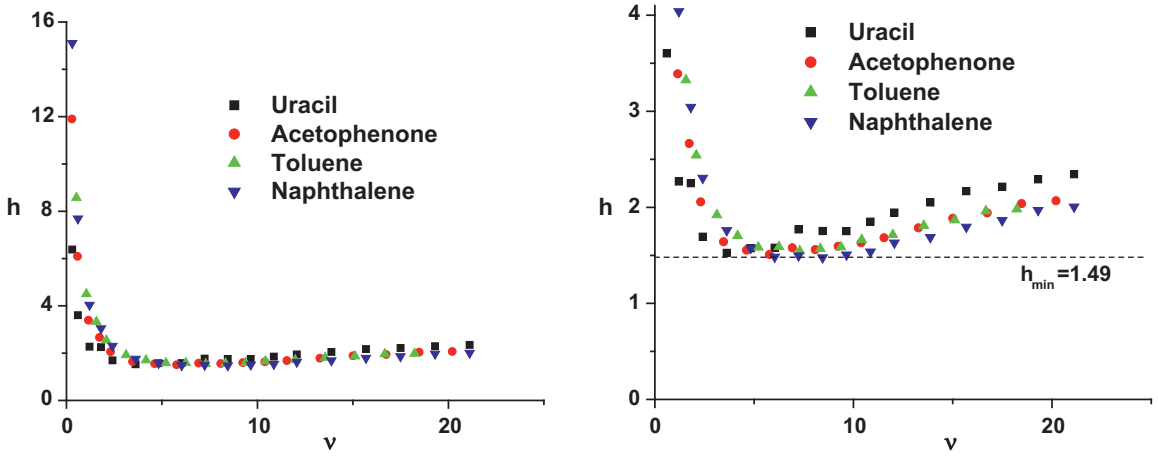

Fig. 18. Plot of the reduced HETP of four small molecules versus the reduced interstitial velocity. Left: HETP measured on a 4.6 mm × 150 mm column packed with 2.6 μm Poroshell120-C_{18} core–shell particles; right: same as in left figure but the plot is zoomed into the minimum range of the HETP plot.Note the minimum reduced plate height of 1.49 and the flat *C* term.

ficient (the C_p coefficient in the legend of this figure), reveals that the access of protein molecules to the internal volume of the particle from the external moving eluent is slower than their diffusivity across the particle. Kinetic limitations to the mass transfer of proteins were alleviated by merely increasing the probability of protein molecules to enter the pore opening on the external surface area of the particle.

- Kinetic properties of Kinetex columns

Fig. 16 (left) shows the reduced plate height plots for the same small molecules as those tested with the Halo column on a 150 mm × 4.6 mm column packed with 2.6 μm Kinetex core–shell particles. Fig. 16 (right) zooms onto the bottom part of this plot, to the minimum reduced HETP. The most striking result in Fig. 16 (left) is the nearly flat C-branch of the reduced plots. In the range of reduced velocities between 5 and 15, the constant decrease of the contribution of axial diffusion is balanced by the slow increase of the combination of the mass transfer and of the eddy diffusion contributions, leaving the reduced HETP practically constant. Fig. 16 (right) shows a minimum reduced HETP of 1.38, a value significantly smaller than those typically observed with fully porous particles ($h_{min} \simeq 2.0$). Additionally, the more retained the compound, the smaller the minimum reduced HETP . This observation indirectly reflects the presence of a significant trans-column velocity bias caused by a slight radial gradient in the local permeability of the column (hence, of its local external porosity) from the center to the wall of the column.

It is noteworthy that the minimum reduced HETP of narrow-bore columns (2.1 mm I.D.) is larger than that of the conventional 4.6 mm I.D. columns. For instance, a 150 mm × 2.1 mm column packed with the same 2.6 μm Kinetex particles as used to pack the 4.6 mm I.D. column in Fig. 14 has a value of h_{min} of about 1.55 (instead of 1.38) or a 15% loss in the column efficiency (see Fig. 17). Worse, if the same narrow-bore column is packed with 1.7 instead of 2.6 μm Kinetex particles, the value of $h_{min} = 2.7$ is found. Such poor values of the reduced HETP of 2.1 mm I.D. columns was reported by several groups [77,100,101].

Regarding the column performance for proteins, the C-branch of the plots is much flatter with Kinetex than with the first generation of Halo 90 Å particles [37,32], which is explained by the larger accessibility of the internal porous volume of the particle mesopores to protein molecules (13% for Kinetex versus 6% for Halo 90 Å) [79].

- Kinetic properties of Poroshell120 columns

The 2.7 μm Poroshell120 core–shell particles were introduced this year by Agilent Technologies. The structure of these particles is very similar to that of the Halo particles manufactured by Advanced Material Technologies with a core size of 1.7 μ. However, the shell layer pore structure is made according to a different proprietary process. For that all, it is not surprising that the reduced HETPs of these two packing materials measured for small molecules are very similar (compare Fig. 18 for Poroshell120 and Fig. 14 for Halo particles). The minimum reduced plate height of the 4.6 mm × 150 mm Poroshell column is 1.49.

As for the Halo and Kinetex materials, the efficiencies of the 2.1 mm I.D. columns are markedly less good than that of the 4.6 mm I.D. columns. Fig. 19 compares the reduced plate heights of naphthalene on 2.1 and 4.6 mm I.D. columns packed with 2.7 μm Poroshell120 particles. The minimum reduced plate heights of these columns are clearly larger for the 2.1 mm than for the 4.6 mm I.D. columns (1.96 for 100 mm long and 2.47 for 50 mm long narrow-bore columns versus 1.49 for a conventional column for naphthalene).

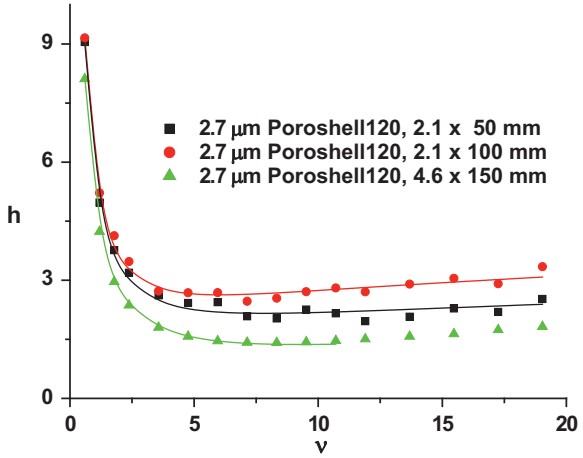

Fig. 19. Comparison between the reduced HETP of naphthalene measured with a 4.6 mm × 150 mm, a 2.1 mm × 100 mm, and a 2.1 mm × 50 mm columns packed with the same 2.7 μm Poroshell120-C_{18} packing material. Note the relatively poor performance of the narrow-bore 2.1 mm I.D. columns. The actual mobile phase flow rate and velocity corresponding to $\nu = 10$ are 1.5 ml/min and 0.38 cm/s, respectively.

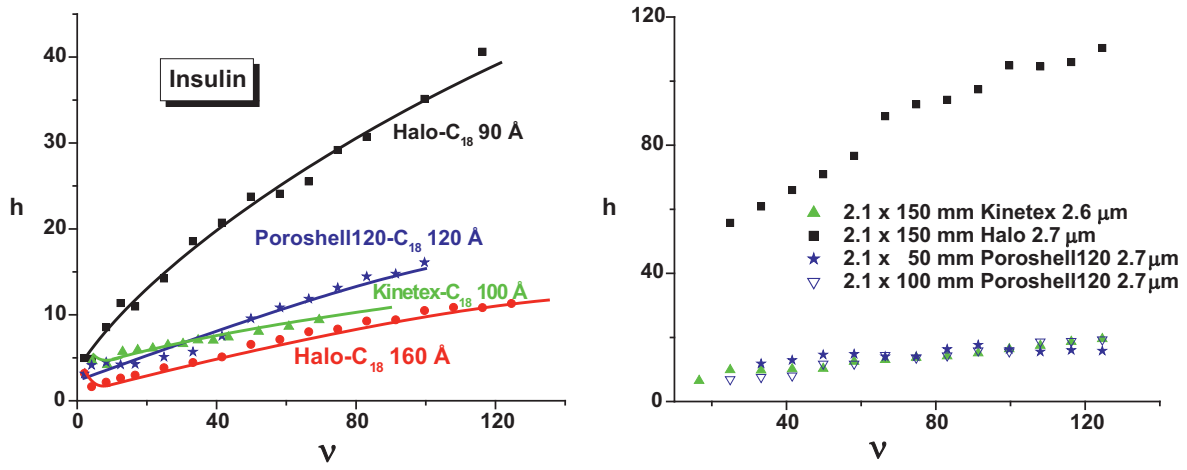

Fig. 20. Left: comparison between the reduced HETP of insulin on 4.6 mm × 150 mm columns packed with 2.7 μm Halo-C_{18} 90 Å (full squares), 2.7 μm Halo-C_{18} 160 Å (full circles), 2.6 μm Kinetex-C_{18} 100 Å (full triangles), and 2.7 μm Poroshell120-C_{18} packing material (full stars). Note the similarity between the performances of the Halo-C_{18} 160 Å, Kinetex-C_{18} 100 Å, and Poroshell120-C_{18} 120 Å columns. The actual mobile phase flow rate and velocity corresponding to $\nu = 10$ are 0.225 ml/min and 0.06 cm/s, respectively. Right: same as in left figure, except the materials were packed in narrow-bore 2.1 mm I.D. columns. Note the equivalent performance of the Kinetex-C_{18} 100 Å and Poroshell120-C_{18} 120 Å columns.

Finally, the mass transfer kinetics of insulin is comparable for the Poroshell120, for the Kinetex, and for the Halo-ES-peptide core–shell particles (see Fig. 20).

- Conclusions

In summary, all available commercial 4.6 mm I.D. columns packed with core–shell particles (Halo, Kinetex, and Poroshell120) exhibit comparable maximum column efficiencies for small molecules, e.g., 240,000, 280,000, and 248,000 plates/m, respectively. The slightly better efficiency of the Kinetex column is mostly due the smaller longitudinal diffusion terms of these columns. This can be explained by the values of the ratios of the core to the particle diameter, 1.9/2.6 = 0.73 for Kinetex and 1.7/2.7 = 0.673 for Halo and Poroshell, respectively. Accordingly, the external volume available for longitudinal diffusion is smaller in the Kinetex column. In contrast there is no simple explanation for lower level of performance achieved with 2.1 mm than with 4.6 mm I.D. columns, which might be explained by the larger impact of the wall effects in the narrow-bore than in the wide I.D. column tubes.

Regarding the mass transfer kinetics of large molecules in these new columns, Fig. 20 compares the experimental reduced plate heights measured for insulin on the columns packed with 2.7 μm Halo 90 Å, 2.6 μm Kinetex 100 Å, 2.7 μm Halo 160 Å, and 2.7 μm Poroshell120 120 Å core–shell particles, all made of regular silica-C_{18} bonded phases packed in 4.6 mm I.D. columns. The content of acetonitrile in the aqueous mobile phase was 32% in all cases. The pH of the eluent was set acidic with the addition of 0.1% (v/v) of trifluoroacetic acid. This figure shows that the C coefficient is nearly the same for all the columns, except for the first generation of 2.7 μm Halo particles. Fig. 21 shows the band profiles recorded at a flow rate of 1.4 ml/min and at room temperature with 1 μl sample injections. The elution of small proteins such as insulin can be performed under isocratic conditions at the high flow rate of 3 ml/min ($\nu = 125$), providing a column efficiency of nearly 35,000 plates per meter, with the 2.7 μm Halo-ES-peptide column. Under gradient elution conditions, the peak shape of insulin is significantly compressed [102–104] and the performance achieved with columns packed with core–shell particles is better than that provided by columns packed with sub-2 μm particles [78,105,106]. Fig. 20 shows the experimental reduced plate heights of insulin on narrow-bore 2.1 mm I.D. columns packed with 2.7 μm Halo 90 Å, 2.6 μm Kinetex 100 Å, and 2.7 μm Poroshell120 120 Å core–shell particles. As expected, the column efficiency is lowest with the 2.7 μm Halo 90 Å. The performances of the Kinetex and Poroshell particles are very similar, with a flat C term. Fig. 20 confirms that higher efficiencies are achieved with wide than with narrow-bore columns, confirming what was observed with small molecules. Fig. 21 compares the experimental elution profiles of insulin on the 2.1 mm × 150 mm Halo column, the 2.1 mm × 150 mm Kinetex column, the 2.1 mm × 100 mm Poroshell column, and the 2.1 mm × 50 mm Poroshell column, with a constant flow rate of 0.30 ml/min, the mobile phase being a mixture of acetonitrile, water, and TFA (32/68/0.1, v/v/v), the temperature 293 K, and the sample size 0.21 μl.

4.2. Mass transfer mechanism in columns packed with modern core–shell particles

In this section, we evaluate and compare the mass transfer mechanism of three 4.6 mm × 150 mm columns packed with 2.6 μm Kinetex, 2.7 μm Halo-C_{18}, and 2.7 μm Halo-ES-peptide core–shell particles. For the sake of comparison, we discuss also the mass transfer mechanisms in a 4.6 mm × 150 mm column packed with 3 μm fully porous Atlantis-C_{18} particles. The strategy followed uses a general experimental protocol aiming at isolating each individual mass transfer terms of the general HETP equation that is described in details elsewhere [48]. These terms include the reduced longitudinal diffusion term (B/ν), the reduced eddy diffusion term ($A(\nu)$), and the trans-particle mass transfer resistance term ($C_p\nu$). The external film mass transfer resistance term ($C_f\nu$) was assumed to be given by the Wilson and Geankoplis correlation [49]. Confidence in this old correlation equation is increased by the results of the validation study performed by Miyabe et al. with porous [52] and non-porous [53] spherical particles, although the size of the particles used in these works was kept significantly larger than sub-3 μm (~15 μm) in order to allow sufficiently precise measurement of the external mass transfer term. After discussing how each of these three mass transfer contributions was measured and determined for the four columns studied, we report on the contribution of frictional heating in the case of columns packed with core–shell particles and the reduced HETP term h_{Heat}.

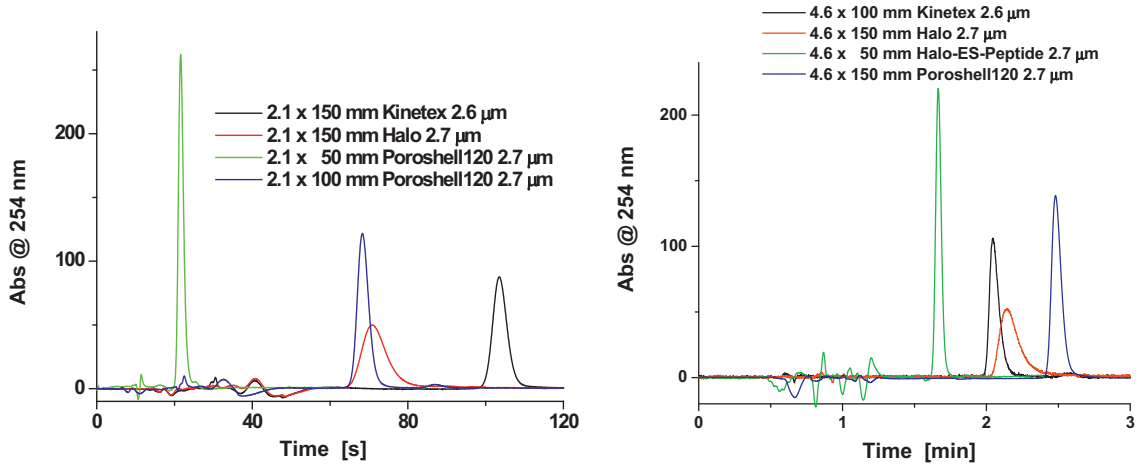

Fig. 21. Comparison between the chromatograms of insulin under linear conditions on narrow-bore 2.1 mm I.D. columns packed with 2.7 µm Halo-C_{18} 90 Å (red), 2.6 µm Kinetex-C_{18} 100 Å (black), and 2.7 µm Poroshell120-C_{18} packing material (green and blue). T = 295 K. Mobile phase: acetonitrile/water/TFA, 32/68/0.1 (v/v/v). Flow rate: 0.30 ml/min. Right: same as in the left figure, except 4.6 mm I.D. columns packed with the same materials. (For interpretation of the references to color in this figure legend, the reader is referred to the web version of this article.)

4.2.1. The B coefficient

The classical B coefficient in the reduced van Deemter plot of h versus the interstitial reduced linear velocity ν was derived from the results of the peak parking method [92,107] performed with four compounds, uracil, acetophenone, toluene, and naphthalene. The use of small molecular weight compounds to measure the B coefficient of packed beds is most convenient due to their relatively high diffusion coefficients ($\simeq 10^{-5}$ cm^2/s). In practice, four parking times (1, 60, 240, and 480 min) were applied and the measurements were performed overnight. Their precision was excellent, with an error of a few percent. In contrast, proteins require longer, more tedious measurements due to their lower diffusion coefficients ($\sim 10^{-6}$ cm^2/s), so parking experiments need several days to a week, which is impractical. The plot of the B coefficient versus the ratio, Ω, of the diffusivity of the sample molecules in the porous part of the particles, D_{eff}, to its bulk diffusion coefficient, D_m, is shown in Fig. 22. The parameter Ω was determined by using the effective medium theory of Landauer [108] adapted by Davis [109] to predict the value of the effective diffusion coefficient of the packed bed.

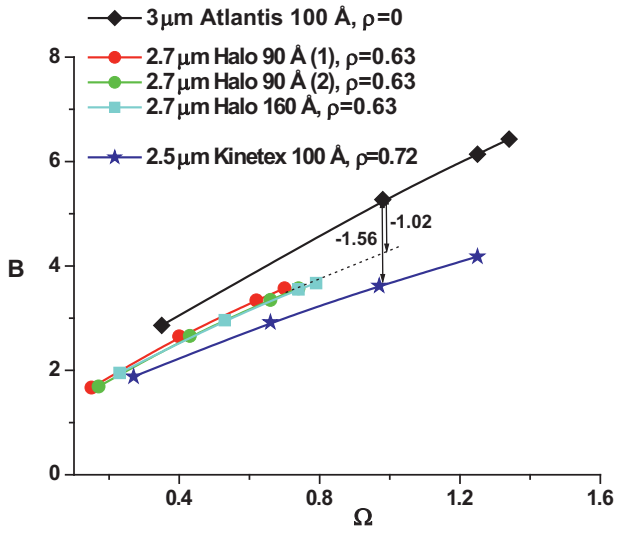

Fig. 22. Plots of the reduced longitudinal diffusion B term versus the ratio of the sample diffusivity, D_{eff}, in the porous shell to the bulk diffusion coefficient, D_m, for fully porous particles (3 µm Atlantis) and superficially porous particles (2.7 µm Halo with ρ = 0.63 and 2.6 µm Kinetex with ρ = 0.72). Note the 20–30% decrease of the B coefficient when the column is packed with core–shell particles.

The consequences of the known differences between the porous structures of the Atlantis-C_{18}, Halo-C_{18}, Halo-ES-peptide-C_{18}, and Kinetex-C_{18} particles are cancelled out in Fig. 22 because the experimental B coefficients are plotted as functions of the ratio Ω. As expected, the presence of a solid core inside the particles has a direct consequence on the B coefficient observed for a column: it decreases by about 20 and 30% when the ratio, ρ, of the core to the particle diameter increases from 0 (Atlantis) to 0.63 (Halo) and to 0.72 (Kinetex), respectively. Accordingly, at the optimum reduced velocity of the column, around 8, the reduced mass transfer contribution (B/ν) decreases from 0.65 (Atlantis) to 0.52 (Halo) and to 0.45 (Kinetex).

In conclusion, the reduced internal porosity of the core–shell particles brings a limited improvement in their efficiency because the longitudinal diffusion coefficient of columns packed with core–shell particles is smaller than that of columns packed with fully porous particles. This causes at best a gain of 0.2 h unit, i.e., a 10% increase in the column efficiency compared to that of columns packed with fully porous particles (h_{min} = 2). Yet, we know (see earlier sections) that the actual gain in column efficiency exceeds 35%. Therefore, another phenomenon must contribute to explain the exceptional performance of the columns packed with core–shell particles.

4.2.2. The C_p coefficient

The theoretical expression for the C_p coefficient with partially porous particles is known for a long time. Horváth and Lipsky [8], Kaczmarski and Guiochon [54], and Felinger [55] used different approaches (configuration factor of the stationary phase, Laplace transform, and probability theory, respectively) to derive it but eventually found the same Eq. 14. The measurement of this coefficient is not straightforward, however, because it requires an accurate model to predict analyte diffusion in the a heterogeneous bed made of porous or superficially porous particles immersed in a liquid phase. In the case of core–shell particles, the difficulty consists in elaborating a physically consistent model of diffusion in a ternary medium made of the non-porous silica cores ($D_1 = 0$), the porous silica shells ($D_2 = D_{\text{eff}} = \Omega D_m$), and the bulk liquid phase ($D_3 = D_m$). The volume fractions occupied by these three media are $(1-\epsilon_e)\rho^3$, $(1-\epsilon_e)(1-\rho^3)$, and $1-\epsilon_e$, respectively. There are only approximate models, such as the parallel diffusion model [110] or

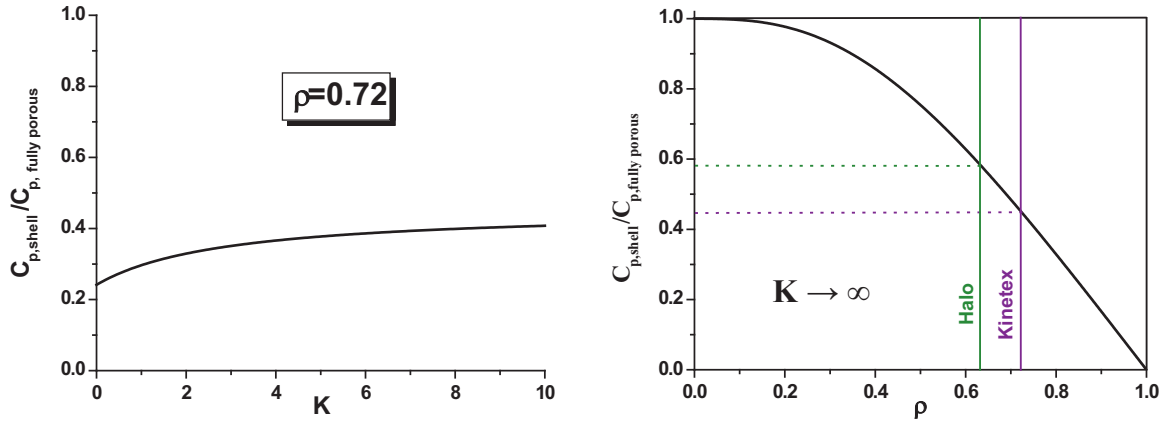

Fig. 23. Left: plots of the C_p coefficient of a core–shell particle with a parameter ρ =0.72, normalized to the C_p coefficient for ρ = 0 as a function of the Henry's constant of adsorption. Right: plots of the C_p coefficient of a core–shell particle for an infinitely retained compound normalized to the C_p coefficient for ρ = 0 as a function of the structural parameter ρ of the particle. Note that for commercialized core–shell particles ($0.63 < \rho < 0.72$) the C_p coefficient is about half that of the same but fully porous particles.

models derived from various effective medium theories [108,109]. The downsides of these models are that they essentially ignore the actual spatial distribution of the three homogeneous media. For retained sample compounds, a recent investigation showed that all these models provide similar estimates of analyte diffusivity inside the porous volume of the particles [111]. Yet, we must emphasize that none of them can be validated because D_{eff} has never been independently measured for small molecules under linear adsorption conditions.

Fig. 23 (left) shows the plot of the ratio of the C_p coefficients of columns packed with core–shell and fully porous particles as a function of the Henry constant K at constant ρ parameter (=0.72, representing the Kinetex particles). Fig. 23 (right) shows a plot of the same C_p ratio as a function of the parameter ρ at constant Henry constant $K \to \infty$. These two graphs demonstrate that the C_p coefficient of commercially available columns packed with core–shell particles ($0.60 < \rho < 0.80$) for moderately to highly retained compounds is typically half that of columns packed with fully porous particles [96].

The actual values of the C_p coefficient are typically between 0.003 and 0.006 for Kinetex [32], Halo, and Halo-ES-peptide [79] for small molecules. Because diffusion is increasingly hindered with increasing molecular size of analytes, the C_p coefficient of insulin is equal to 0.015, 0.035, and 0.022 with Kinetex, Halo, and Halo-ES-peptide particles, respectively. Yet, the overall C terms measured for insulin are much larger than C_p, at 0.060, 0.300, and 0.085.

In conclusion, the C-branch of the van Deemter curve is mostly accounted for by the external film mass transfer resistance across the thin layer of eluent surrounding the external surface area of the particles.

4.2.3. The A term

The measurement of the sole contribution of eddy diffusion is a delicate process. This term accounts for all the sources of flow heterogeneity taking place at any scale length inside the chromatographic column, from the inter-particle distance ($\simeq(d_p/6)$) to the column diameter, through the whole range of trans-channel and inter-channel distances. Accordingly, some experimental strategies must be elaborated in order to subtract from experimental HETP data the contributions of longitudinal diffusion, trans-particle diffusion, and external film mass transfer resistance.

As a first attempt, HETP data were measured by blocking the analyte access to the mesopores by filling them with n-nonane, which wets the pores of silica-C_{18} particles. Pure water was used as the eluent and thiourea as the analyte. The advantage of using thiourea is that it does not partition between n-nonane trapped inside the mesopores and the interstitial eluent [111,112]. However, it was concluded that the eddy diffusion term measured by this method is systematically larger than the one that takes place in the same column when the mesopores are accessible to the eluent because diffusion through the mesopores of the particles contributes to efficiently relax the concentration gradients across the column [98,113]. As a result, the pore blocking method was abandoned.

In a second approach, the eddy diffusion term was derived by subtraction of the sum of the longitudinal diffusion (see Section 4.2.1) and the trans-particle mass transfer resistance terms (see Section 4.2.2) from the overall column reduced HETP, h, measured separately. The external film mass transfer term was estimated from the Wilson and Geankoplis correlation [114]:

$$h_{Eddy} = h - \frac{B}{\nu} - C_p\nu - C_f\nu \tag{18}$$

Fig. 24 (left and right) compares the plots versus the reduced velocity of the eddy diffusion terms of moderately retained compounds (acetophenone and toluene) measured for the Atlantis-C_{18} column (fully porous particles) and the Kinetex-C_{18} column. Strikingly, the eddy diffusion terms of the column packed with core–shell particles is significantly smaller (−40%) than that of the column packed with fully porous particles. The difference becomes most important in the high velocity range but is quite significant at the plate height minimum ($\nu \simeq 8$). The values of the reduced eddy diffusion term are typically 0.9 and 1.5 with columns packed with core–shell and totally porous particles, respectively.

In conclusion, the exceptional performance of columns packed with core–shell particles is first and foremost due to the small eddy diffusion term observed for these columns. It is still unclear whether this is due to the size distribution of these particles (RSD of 5%) which is narrower than that of fully porous particles (RSD of 15%). Theoretical calculations have shown that the size distribution of particles has little impact (∼0.1 h unit on the sample dispersion provided the external porosity of the bed was the same [115]. Even worse, these calculations predict that the eddy diffusion terms of packed beds having an external porosity of 0.366 (which are representative of beds packed with fully porous particles) should be smaller than that of beds having an external porosity of 0.40 (which are typical of beds packed with core–shell particles). On the other hand, the very few experimental results available [116–118] suggest unambiguously that narrower particle size distributions do not potentially provide higher column efficiencies. In fact, it is quite plausible that the trans-column eddy diffusion term is smaller

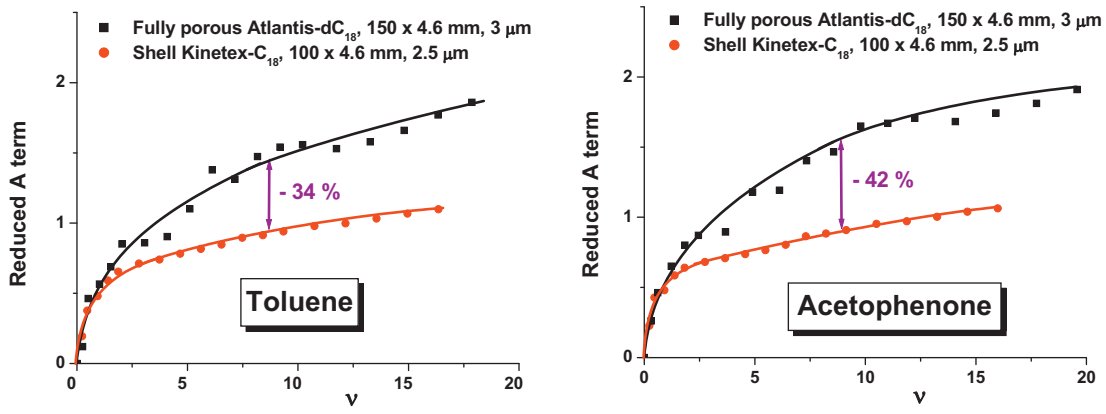

Fig. 24. Left: plots of the reduced eddy diffusion term *A* of toluene measured with two columns, one packed with fully porous particles (3 µm Atlantis-C_{18}), the second with core–shell particles (2.6 µm Kinetex core–shell particles). Note the lower *A* term (−35%) of the column packed with core–shell particles. Right: same plots, on the same columns as in the left figure, but for acetophenone.

for columns packed with core–shell than with fully porous particles because they provide more homogeneous packed beds with lesse strain distributions, due to their rougher external surface [32,96,119] (see Section 4.1.3). Independent measurements by local electrochemical detection of the profiles of bands eluted from a 4.6 mm I.D. column packed with Halo particles have confirmed this assumption [32,99].

4.2.4. The h_{Heat} term

Frictional heating generates heat everywhere across the column, resulting in a heterogeneous temperature distribution along and across it, which can severely decrease its efficiency when the product of the flow rate by the pressure gradient along the column, e.g., the power of heat friction generated exceeds 4 W/m when the column is kept under still-air conditions and pure acetonitrile is used as the eluent [120]. The additional reduced plate height due to this frictional heating was investigated from theoretical and experimental point, of view [56,120–130].

This additional HETP term was measured for narrow-bore columns (2.1 mm × 150 mm) packed with 1.7 µm Kinetex-C_{18} core–shell particles and with BEH-C_{18} fully porous particles. Fig. 25 compares the experimental and theoretical variations of h_{Heat} with the reduced velocity. It shows that the large h_{Heat} values observed with the BEH particles is directly related to the smaller heat conductivity of a bed packed with BEH-C_{18} ($\lambda_{BEH} \simeq 0.30$ W/m/K) than that of a bed packed with Kinetex ($\lambda_{BEH} \simeq 0.70$ W/m/K) particles [127,128]. As a result, the radial temperature gradients are markedly larger across the BEH column than across the Kinetex column. The difference between the thermal conductivities of the two columns is due to the thermal conductivity of the solid silica core (1.4 W/m/K) being much larger than that of porous silica impregnated with an organic eluent like acetonitrile.

5. Possible future developments of modern core–shell particles

As results from previous discussions in this paper, the advantages in terms of efficiency of the columns packed with core–shell particles over those packed with fully porous particles are threefold for small molecular weight analytes:

- The longitudinal diffusion *B* term is lower by about −25% when the ratio of the core to the particle diameters is around 0.7, as it is with commercial core–shell particles. This accounts for a 10% increase of the column efficiency at the optimum velocity.
- The eddy diffusion *A* term is decreased by about −40%, which contributes to most of the increase of the column efficiency.
- The trans-particle mass transfer resistance is reduced by a factor 2. However, its impact on this improvement of the column efficiency is generally negligible.

Regarding the analysis of high-molecular-weight compounds (such as proteins), the benefit of using colimns packed with core–shell versus totally porous particles is less obvious because the mass transfer kinetics of these compounds is mostly controlled by the average mesopore size of the porous shell and by the ease of access of molecules into the porous shell [79,96].

Possible future improvements in the core–shell particles and column packed with them in order to improve the efficiency of these columns could address the optimization of the shell thickness, of the porous shell, and of their packing process.

5.1. Decreasing the shell thickness

It would appear attractive to decrease the thickness of the porous shell in order reduce the *B* and C_p coefficients. Yet, the slurry packing of nearly non-porous or completely non-porous particles requires higher pressures and tends to provide less homogeneous

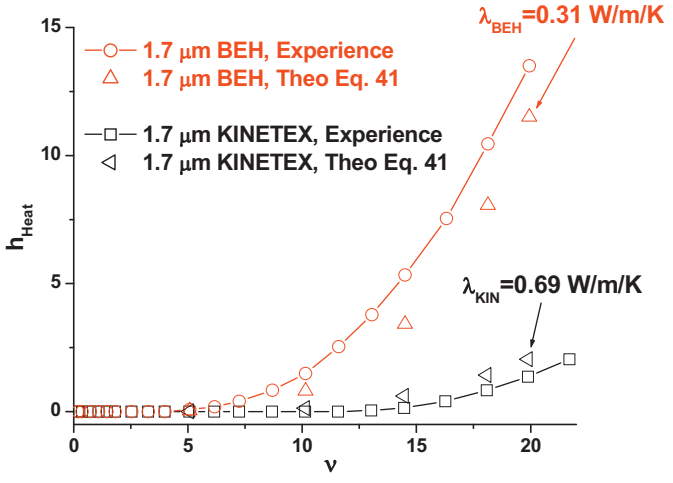

Fig. 25. Plots of the reduced plate height term, h_{Heat}, related to the sole effect of frictional heating on the overall reduced plate height of narrow-bore columns (2.1 mm × 150 mm) packed with fully porous (1.7 µm BEH particles) and core–shell particles (1.7 µm Kinetex particles). Note the very limited impact of frictional heating with columns packed with core–shell particles relatively to those packed with fully organic/inorganic hybrid particles. The difference is accounted for by the larger heat conductivity of the bed packed with core–shell Kinetex-C_{18} particles (λ_{KIN} = 0.69 W/m/K) than that packed with BEH-C_{18} particles (λ_{BEH} = 0.31 W/m/K).

beds, exhibiting lesser efficiency than beds of fully porous particles. Furthermore, reducing the shell thickness might affect the column loadability, reducing the acceptable sample size and reducing detection sensitivity. The problem is as follows:

Consider a chromatographic column containing a fixed number of N core–shell particles, with ρ the core-to-particle diameter ratio. N depends only on the particle-to-column volume ratio. The total surface area available for adsorption inside the column, $S(\rho)$, is given by:

$$S_{\text{ads}}(\rho) = (1-\rho^3)S_{\text{ads}} \tag{19}$$

where S_{ads} is the surface area available within a fully porous particle. The elution volume under linear conditions is:

$$V_R(\rho) = [\epsilon_e + (1-\epsilon_e)(1-\rho^3)\epsilon_p]V_c + (1-\rho^3)S_{\text{ads}}K \tag{20}$$

where V_c is the column tube volume and K is the equilibrium ratio or Henry constant, i.e., the ratio of the surface concentration (mol/m^2) to the bulk volume concentration (mol/m^3) at equilibrium. Accordingly:

$$K = \frac{V_0}{S_{\text{ads}}}\frac{n_{\text{ads}}}{n_b} = \frac{k}{F'} \tag{21}$$

where $F' = S_{\text{ads}}/V_0$ is the phase ratio or ratio of the stationary surface to the mobile phase volumes while n_{ads} and n_b are the numbers of analyte molecules that are adsorbed onto the surface and are dissolved in the bulk phase at equilibrium, respectively. F' has the unit of a reciprocal length. We assume that K is the same whether the particle is fully or partially porous. It is a property of the porous shell of the particle, only, and has the dimension of a length.

Now, let the structural parameter ρ increase by the amount $d\rho$. By how much should the equilibrium constant K change so that the retention volume V_R remains constant? Differentiating Eq. 20 with respect to ρ gives

$$\frac{S_{\text{ads}}dK}{\epsilon_p(1-\epsilon_e)V_c + S_{\text{ads}}K} = \frac{3\rho^2}{1-\rho^3}d\rho \tag{22}$$

The separation of the variables K and ρ followed by integration from $\rho = 0$ to ρ gives:

$$K(\rho) = \frac{\epsilon_p(1-\epsilon_e)V_c}{S_{\text{ads}}}\left(\frac{\rho^3}{1-\rho^3}\right) + \frac{1}{1-\rho^3}K(\rho=0) \tag{23}$$

Eq. (23) demonstrates that if the retention volume of a compound on a column packed with core–shell particles must remain constant and equal to the retention volume on a column packed with fully porous particles, in order to keep the same resolution and peak capacity under isocratic and gradient elution modes, the equilibrium constant between the surface of the adsorbent and the eluent must be increased. For instance, the modifier concentration in water must be decreased in RPLC. This could eventually cause serious problems, enhancing column overloading effects or even peak tailing when the adsorbent surface is heterogeneous [87,89,90,131,132].

For a chromatographic system having an apparent efficiency of N plates/m and a Langmuir adsorption isotherm, thermodynamic overloading effects begin to distort the Gaussian peak shape into a Langmuirian one when [41]:

$$\frac{bc_0}{1+bc_0} > p(N)\% \tag{24}$$

where p is an arbitrary limit which essentially depends on the system efficiency (typically $p = 5\%$ for $N = 250{,}000$ plates per meter, see Fig. 26) and b is the equilibrium constant given by:

$$b = \frac{K}{n_{\max}/S_{\text{ads}}} = \frac{K}{q_S} \tag{25}$$

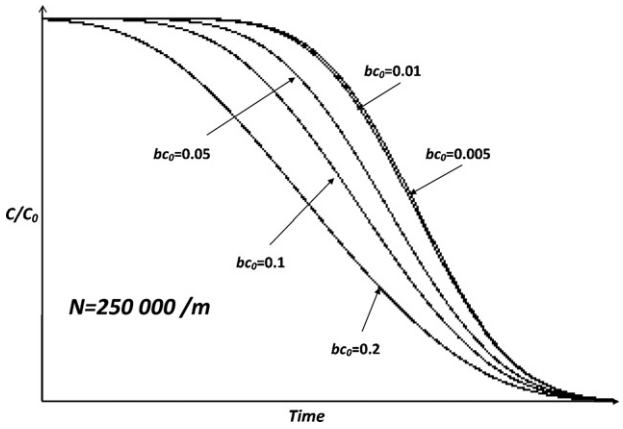

Fig. 26. Impact of the thermodynamic effect measured by the product of the equilibrium constant b by the bulk concentration c_0 on the distortion of the rear part of a breakthrough profile. Langmuir isotherm with $q_S = 1$ g/L and $b = 0.1$ L/g. Column length $L = 10$ cm and efficiency $N = 25{,}000$.

where $n_{\max}$ is the maximum sample size (in mole) that can be adsorbed onto the surface of the porous particles. q_S is the saturation capacity of the porous silica in mol/m^2. According to the condition (24), this sets an upper limit for the structural parameter ρ defined by:

$$K(\rho) < \left(\frac{1-p}{p}\right)\frac{q_S}{c_0} \tag{26}$$

For a column with $V_c = 2.5$ cm^3 (150 mm × 4.6 mm I.D. column), $\epsilon_e = 0.4$, $\epsilon_p = 0.4$. Therefore, $V_0 = 1.6$ cm^3, the mass of silica inside the column is 2.0 g (density 2.2 g/cm^3), and the surface available is $S_{\text{ads}} = 200 \times 10^4$ cm^2 (100 m^2/g with average mesopore size of 120 Å). The saturation capacity, q_S, for small organic molecules are typically around 100 g/L [89] or 4.5×10^{-6} g/cm^2. The concentration of the sample is usually taken at $c_0 = 0.001$ g/cm^3, p is 10% and N 250,000 plates/m. Finally consider an initial retention factor $k(\rho = 0) = 5$. The condition Eq. (24) can now be written as:

$$\epsilon_p(1-\epsilon_e)\left[\frac{k(\rho=0)+\rho^3}{1-\rho^3}\right] + \frac{\epsilon_e k(\rho=0)}{1-\rho^3} < \left(\frac{1-p}{p}\right)\frac{q_S}{c_0}\frac{S_{\text{ads}}}{V_c} \tag{27}$$

This leads to two conclusions

- If the adsorption process is homogeneous, Eq. 27 is always satisfied even with non porous particles. There is no risk of concentration overload unless $\rho > 0.99996$.
- Most likely, particularly with polar and ionizable compounds in RPLC, the saturation capacity of the most active sites is two to four order magnitude less than the total saturation capacity [89]. For instance, if $q_S = 1$, 0.1, and 0.01 g/L, then ρ should be kept smaller than 0.996, 0.96, and 0.22, respectively.

Whether thinner shell should be prepared or not depends on the degree of heterogeneity of the adsorption process of the compounds concerned and on the saturation capacity of the most active sites on the adsorbent surface. In most cases and for small neutral compounds in RPLC for which the saturation capacity of the most active sites is always larger than 1 g/L, there is no great risk of severe column overloading.

As far as large molecules are concerned, decreasing the shell thickness is, in theory, highly advantageous as shown in Fig. 27 and demonstrated in [133]. Because the diffusivity of large molecules through the porous shell is severely hampered (limited accessible porosity and significant pore diffusion hindrance), shortening the diffusion path across the particles will significantly decrease the

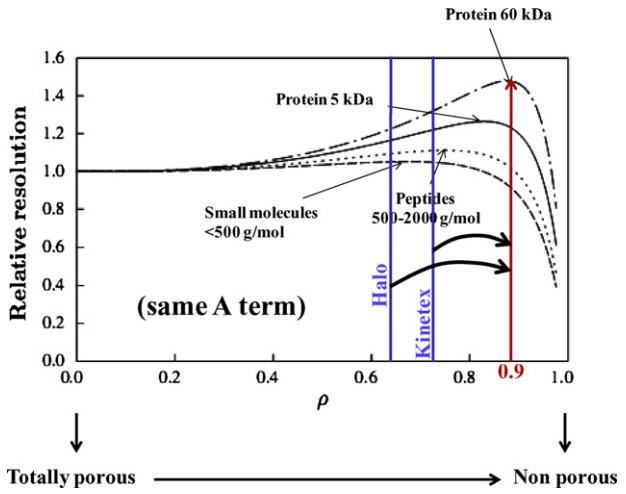

Fig. 27. Plots of the relative resolution of columns packed with core–shell particles (with respect to the resolution of the same column packed with fully porous particles) as a function of the structural shell parameter ρ (from fully porous particles, e.g., $\rho = 0$, to non-porous particles, e.g., $\rho = 1$ for small molecules ($M < 500$ g/mol), peptides ($500 < M < 2000$), small proteins (insulin, $M = 5$ kDa), and large proteins (BSA, $M = 60$ kDa)).

C_p coefficient. Theory predicts that the optimum core-to-particle diameter ratio should be around 0.85 and 0.90 for insulin (5 kDa) and bovine serum albumin (60 kDa), respectively. This decrease in shell thickness could potentially lead to an increase of the relative resolution (with respect to fully porous particles) of 30 and 50%, respectively.

Surprisingly, despite the obvious advantages expected, no sub-3 μm core–shell particles with a large ratio ρ in the range 0.8–0.95 have yet been introduced. This might be because packing nearly non-porous sub-3 μm particles is uneasy. In fact, we showed that the trans-column velocity biases are more efficiently relaxed when the particles are porous than when they are not [98,112]. A compromise between a decrease of the *B* term and the increase of the *A* term has to be found and the best optimum particle size seem to correspond to ρ values in the range of 0.6–0.7.

5.2. Packing efficiently sub-2 μm core–shell particles

A last possible development for core–shell particles would consist in finding ways to more effectively pack narrow-bore columns with sub-2 μm core–shell particles. Such particles do exist but the chromatographic performance of these columns was found to be disappointing, merely equivalent to that of columns packed with sub-2 μm conventional fully porous particles [77,127,128].

Would manufacturers be able to produce narrow-bore columns with a reduced HETP of 1.5 (as they do today with 2.6 μm particles packed into 4.6 mm I.D. column), plate height of 2.5 μm and plate counts of 400,000 plates/m would become a reality. Yet, the full potential of these columns could not become a reality unless better instruments, with smaller extra-column contributions be designed in the near future.

6. Conclusions

This review demonstrates how successful is the rebirth of the old core–shell particle technology imagined in the late 1960s for 50 μm particles (with a shell thickness of a few micron) and recently re-introduced into the field as the sub-3 μm particles (with a shell thickness of a few hundreds nanometer). The preparation of thin porous shells (thickness from 250 to 500 nm) around spherical non-porous silica cores (diameter from 1.2 to 1.7 μm) can now be well controlled. It has been patented by manufacturers. While the aggregation of silica nano-particles was used to form the porous shells of the large precursor core–shell particles (average pore size ≃1000 Å), the repetition of the templating agent synthesis route is now used to generate average pore sizes of ≃100 Å within porous silica. As a result, the formation of thick shells containing small mesopores around small cores provides a new generation of core–shell particles which have a specific surface area comparable to that of the conventional fully porous silica particles prepared by a sol–gel process. The limitation of the old core–shell particles that was related to their poor sample loadability is completely overcome. Most of the success of this generation of sub-3 μm particles lies in the unexpectedly low minimum reduced plate height of their packed columns, in the range of 1.2–1.5 instead of 2.0 for the same columns packed with fully porous particles.

Strikingly, the exceptional performance of 4.6 mm I.D. columns packed with the last generation of sub-3 μm core–shell particles is not caused by the reduction of the sample diffusion path across these particles (smaller *C* term), which was the initial incentive for commercializing core–shell particles since the early 1970s. If this were true, the minimum reduced plate height for small molecules would be decreased by only 0.05 h unit, a marginal gain in column efficiency. The actual advantages of columns packed with these new core–shell particles lie in the diminution of both the longitudinal diffusion *B* coefficient (− 20 to −30%) and the eddy diffusion *A* term (−40%). The decrease of the *B* coefficient was expected because a significant fraction of the column volume (≃20%) is now occupied by non-porous silica through which analytes cannot axially diffuse. In contrast, the diminution of the eddy diffusion term was unexpected. It remains uncertain whether the significant decrease of the *A* term is caused by the tighter size distribution of core–shell (5–7%) versus fully porous (15–20%) particles (decrease of the short-range inter-channel velocity biases) or by the decrease of the trans-column velocity biases caused by the visible roughness of the external surface area of the core–shell particles.

Minimum plate heights as low as 3 μm have already been observed in 4.6 mm I.D. columns with 2.6 μm core–shell particles. This achievement constitutes a challenge for the manufacturers of standard (<400 bar) chromatographs the contributions of which to the overall band broadening is seriously affecting the quality of the separations. New injection systems, narrower connecting tubes, and smaller detection cell volumes are definitely required. Would the manufacturers of core–shell particles be soon able to pack narrow-bore columns as well as they do 4.6 mm I.D. columns, major changes in instrumentation design would become urgently needed. Interestingly, however, the development of the improved structures of core–shell particles has not reached an end and much remains to be done to improve the mass transfer of large molecules.

The advent of the last generation of sub-3 μm core–shell particles has suddenly raised two important issues in the research and development of more performing LC separation systems:

- How to pack efficiently narrow-bore columns with dense sub-2 μm core–shell particles?
- How to reduce significantly the contributions of the latest state of the art very-high pressure LC instruments while keeping a large range of flow rates?

Manufacturers of columns and instruments are already deeply involved in these developments. Today, the performance of columns is more advanced than that of LC instruments. We expect a new generation of LC instruments susceptible to allow analysts to maximize the resolution of his sample.

Acknowledgements

This work was supported in part by grant CHE-06-08659 of the National Science Foundation and by the cooperative agreement between the University of Tennessee and the Oak Ridge National Laboratory. We thank Tivadar Farkas (Phenomenex, Torrance, USA) for the generous gift of the Kinetex columns used in our work and for fruitful discussions, Jack Kirkland for the generous gift of the Halo and Halo-ES-peptides columns used in our work and for fruitful discussions, and Ron Majors (Agilent, Little Falls, and DE) for the generous gift of the Poroshell120 columns used in our work, for the gift of the last flasks of Zipax packing material, and for fruitful discussions.

References

[1] M.S. Tswett, Tr. Protok. Varshav. Obshch. Estestvoistpyt. Otd. Biol. 14 (1903, publ. 1905) 20; and in "On the New Category of Adsorption Phenomena and their Applications in Biochemical Analysis". Reprinted and Translated in G. Hesse and H. Weil, "Tswett's erste chromatographische Schrift", Woelm, Eschwegen, 1954.
[2] M.S. Tswett, Ber. Deut. Bot. Ges. 24 (1906) 316.
[3] M.S. Tswett, Ber. Deut. Bot. Ges. 24 (1906) 384.
[4] J.J. Kirkland, Modern Practice of Liquid Chromatography, J. Wiley, New York, 1971.
[5] J.R. Parrish, Nature 207 (1965) 402.
[6] J.H. Knox, Anal. Chem. 38 (1966) 253.
[7] C.G. Horváth, B.A. Preiss, S.R. Lipsky, Anal. Chem. 39 (1967) 1422.
[8] C. Horváth, S.R. Lipsky, J. Chromatogr. Sci. 7 (1969) 109.
[9] J.J. Kirkland, J. Chromatogr. Sci. 7 (1969) 7.
[10] J.J. Kirkland, US patent 3,505,785 (1969).
[11] J.J. Kirkland, Anal. Chem. 41 (1969) 218.
[12] J.F.K. Huber, J. Chromatogr. Sci. 9 (1971) 72.
[13] J.F.K. Huber, C.A.M. Meijers, J.A.R. Hulsman, Anal. Chem. 44 (1972) 111.
[14] I. Halasz, H. Englehardt, J. Asshauer, B.L. Karger, Anal. Chem. 42 (1970) 1460.
[15] B.L. Karger, L.V. Berry, Clin. Chem. 17 (1971) 757.
[16] J.J. Kirkland, Anal. Chem. 64 (1992) 1239.
[17] J.N. Done, J.H. Knox, J. Chromatogr. Sci. 10 (1972) 606.
[18] J.N. Done, G.J. Kennedy, J.H. Knox, Gas Chromatogr. 1973 (1973) 145.
[19] J.H. Knox, Anal. Chem. 38 (1966) 253.
[20] I. Halasz, M. Naefe, Anal. Chem. 44 (1972) 76.
[21] I. Halasz, H. Englehardt, J. Asshauer, B.L. Karger, Anal. Chem. 42 (1970) 1460.
[22] L. Jelinek, P. Dong, C. Rojas-Pajos, H. Taïbi, E. sz Kovats, Langmuir 8 (1992) 2152.
[23] M. Kele, G. Guiochon, J. Chromatogr. A 830 (1999) 41.
[24] M. Kele, G. Guiochon, J. Chromatogr. A 830 (1999) 55.
[25] M. Kele, G. Guiochon, J. Chromatogr. A 855 (1999) 423.
[26] M. Kele, G. Guiochon, J. Chromatogr. A 869 (2000) 181.
[27] A. Felinger, M. Kele, G. Guiochon, J. Chromatogr. A 913 (2001) 23.
[28] M. Kele, G. Guiochon, J. Chromatogr. A 913 (2001) 89.
[29] J.J. Kirkland, T.J. Langlois, US patent application 20070189944 a1 (2007).
[30] J.J. Kirkland, T.J. Langlois, J.J. DeStefano, Am. Lab. 39 (8) (2007) 18.
[31] J.J. DeStefano, T.J. Langlois, J.J. Kirkland, J. Chromatogr. Sci. 46 (2007) 254.
[32] F. Gritti, I. Leonardis, J. Abia, G. Guiochon, J. Chromatogr. A 1217 (2010).
[33] F.C. Leinweber, U. Tallarek, J. Chromatogr. A 1006 (2003) 207.
[34] K. Mihlbachler, T. Kollmann, A. Seidel-Morgenstern, J. Tomas, G. Guiochon, J. Chromatogr. A 818 (1998) 155.
[35] B.G. Yew, J. Ureta, R.A. Shalliker, E.C. Drumm, G. Guiochon, AIChE J. 49 (2003) 642.
[36] T. Farkas, G. Zhong, G. Guiochon, J. Chromatogr. A 849 (1999) 35.
[37] F. Gritti, I. Leonardis, D. Shock, P. Stevenson, A. Shalliker, G. Guiochon, J. Chromatogr. A 1217 (2010) 1589.
[38] G. Guiochon, J. Chromatogr. A 1126 (2006) 6.
[39] R.B. Bird, W.E. Stewart, E.N. Lightfoot, Transport Phenomena, J. Wiley, New York, 1962.
[40] J.C. Giddings, Dynamics of Chromatography, Marcel Dekker, New York, NY, 1960.
[41] G. Guiochon, A. Felinger, A.M. Katti, D.G. Shirazi, Fundamentals of Preparative and Nonlinear Chromatography, Elsevier, Amsterdam, The Netherlands, 2006.
[42] J.C. Sternberg, Adv. Chromatogr. 2 (1966) 205.
[43] F. Gritti, C.A. Sanchez, T. Farkas, G. Guiochon, J. Chromatogr. A 1217 (2010) 3000.
[44] F. Gritti, G. Guiochon, J. Chromatogr. A 1217 (2010) 7677.
[45] F. Gritti, G. Guiochon, J. Chromatogr. A (2011).
[46] A. Felinger, G. Guiochon, J. Chromatogr. A 913 (2001) 221.
[47] B. Lin, G. Guiochon, Modeling for Preparative Chromatography, Elsevier, Amsterdam, The Netherlands, 2003.
[48] F. Gritti, G. Guiochon, J. Chromatogr. A 1217 (2010) 5137.
[49] E.J. Wilson, C.J. Geankoplis, J. Ind. Eng. Chem. (Fundam.) 5 (1966) 9.
[50] K. Miyabe, M. Ando, N. Ando, G. Guiochon, J. Chromatogr. A 1210 (2008) 60.
[51] K. Miyabe, Y. Kawaguchi, G. Guiochon, J. Chromatogr. A 1217 (2010) 3053.
[52] K. Miyabe, M. Ando, N. Ando, G. Guiochon, J. Chromatogr. A 1210 (2008) 60.
[53] K. Miyabe, Y. Kawaguchi, G. Guiochon, J. Chromatogr. A 1217 (2010) 3053.
[54] K. Kaczmarski, G. Guiochon, Anal. Chem. 79 (2008) 4648.
[55] A. Felinger, J. Chromatogr. A 1218 (2011) 1939.
[56] J. Kotska, F. Gritti, G. Guiochon, K. Kaczmarski, J. Chromatogr. A 1217 (2010) 4704.
[57] F. Gritti, G. Guiochon, J. Chromatogr. A, submitted for publication.
[58] K.K. Unger, G. Jilge, J.N. Kinkel, M.T.V. Hearn, J. Chromatogr. 359 (1986) 61.
[59] J.J. DeStefano, T.J. Langlois, J.J. Kirkland, J. Chromatogr. Sci. 46 (2008) 254.
[60] K. Kalghatji, C. Horváth, J. Chromatogr. 398 (1987) 335.
[61] R.K. Iler, The Chemistry of Silica, J. Wiley, New York, 1979.
[62] J.J. Kirkland, J. Chromatogr. Sci. 7 (1969) 361.
[63] J.J. Kirkland, J. Chromatogr. Sci. 10 (1972) 129.
[64] G.J. Kennedy, J.H. Knox, J. Chromatogr. Sci. 10 (1972) 549.
[65] F. Gritti, G. Guiochon, AIChE J. 56 (2010) 1495.
[66] J.J. Kirkland, J. Chromatogr. Sci. 8 (1970) 72.
[67] J.J. Kirkland, J. Chromatogr. Sci. 9 (1971) 206.
[68] J.J. Kirkland, J.J. DeStefano, J. Chromatogr Sci. 8 (1970) 309.
[69] J.A. Schmit, R.A. Henry, R.C. Williams, J.F. Dieckman, J. Chromatogr. Sci. 9 (1971) 645.
[70] H.C. Beachell, J.J. DeStefano, J. Chromatogr. Sci. 10 (1973) 481.
[71] J.H. Knox, G. Vasvari, J. Chromatogr. 83 (1973) 181.
[72] X. Wang, W.E. Barber, P.W. Carr, J. Chromatogr. A 1107 (2006) 139.
[73] X. Wang, D.R. Stoll, A.P. Schellinger, P.W. Carr, Anal. Chem. 78 (2006) 3406.
[74] J. Urban, P. Jandera, Z. Kucerová, M.A. van Straten, H.A. Claessens, J. Chromatogr. A 1167 (2007) 63.
[75] F. Gritti, G. Guiochon, J. Chromatogr. A 1157 (2007) 289.
[76] F. Gritti, A. Cavazzini, N. Marchetti, G. Guiochon, J. Chromatogr. A 1157 (2007) 289.
[77] E. Oláh, S. Fekete, J. Fekete, K. Ganzler, J. Chromatogr. A 1217 (2010) 3642.
[78] F. Gritti, G. Guiochon, J. Chromatogr. A 1217 (2010) 1604.
[79] F. Gritti, G. Guiochon, J. Chromatogr. A 1218 (2011) 907.
[80] H. Geische, J. Eur. Ceram. Soc. 14 (1994) 205.
[81] W. Stober, A. Fink, E. Bohn, J. Colloid Interface Sci. 26 (1968) 62.
[82] S.B. Yoon, J.-Y. Kim, J.H. Kim, Y.J. Park, K.R. Yoon, S.K. Park, J.-S. Yu, J. Mater. Chem. 17 (2007) 1758.
[83] J.H. Kim, S.B. Yoon, J.-Y. Kim, Y.B. Chae, J.-S. Yu, Colloid Surf. A: Physicochem. Eng. Aspects 313–314 (2008) 77.
[84] Y. Ma, L. Qi, J. Ma, Y. Wu, O. Liu, H. Cheng, Colloids Surf. A: Physicochem. Eng. Aspects 229 (2003) 1.
[85] D. Cabooter, A. Fanigliulo, G. Bellazzi, B. Allieri, A. Rottigni, G. Desmet, J. Chromatogr. A 1217 (2010) 7074.
[86] A. Daneyko, S. Khirevich, U. Tallarek, in: 35th International Symposium and Exhibit on High Performance Liquid Phase Separations and Related Techniques, HPLC2006, San Francisco, June 17–22, 2006.
[87] F. Gritti, G. Guiochon, J. Chromatogr. A 1028 (2004) 75.
[88] F. Gritti, G. Guiochon, Anal. Chem. 77 (2005) 1020.
[89] F. Gritti, G. Guiochon, J. Chromatogr. A 1099 (2005) 1.
[90] F. Gritti, G. Guiochon, Anal. Chem. 78 (2006) 5823.
[91] F. Gritti, G. Guiochon, J. Chromatogr. A 1115 (2006) 142.
[92] F. Gritti, G. Guiochon, Chem. Eng. Sci. 61 (2006) 7636.
[93] F. Gritti, G. Guiochon, J. Chromatogr. A 1161 (2007) 157.
[94] F. Gritti, G. Guiochon, J. Chromatogr. A 1169 (2007) 111.
[95] I. Rustamov, T. Farcas, F. Ahmed, F. Chan, R. LoBrutto, H.M. McNair, Y.V. Kazakevich, J. Chromatogr. A 913 (2001) 49.
[96] F. Gritti, G. Guiochon, J. Chromatogr. A 1217 (2010) 8167.
[97] F. Gritti, G. Guiochon, J. Chromatogr. A 1218 (2011) 1592.
[98] F. Gritti, G. Guiochon, J. Chromatogr. A 1217 (2010) 6350.
[99] J.A. Abia, K.S. Mriziq, G. Guiochon, J. Chromatogr. A 1216 (2009) 3185.
[100] Y. Zhang, X. Wang, P. Mukherjee, P. Petersson, J. Chromatogr. A 1216 (2010) 4597.
[101] D.V. McCalley, J. Chromatogr. A 1217 (2010) 4561.
[102] F. Gritti, G. Guiochon, J. Chromatogr. A 1212 (2008) 35.
[103] F. Gritti, G. Guiochon, J. Chromatogr. A 1215 (2008) 64.
[104] F. Gritti, G. Guiochon, J. Chromatogr. A 1216 (2009) 6124.
[105] S.A. Schuster, B. Wagner, B. Boyes, J. Kirkland, J. Chromatogr. Sci. 48 (2010) 566.
[106] J. Salisbury, J. Chromatogr. Sci. 46 (2008) 883.
[107] K. Miyabe, Y. Matsumoto, G. Guiochon, Anal. Chem. 79 (2007) 1970.
[108] R. Landauer, J. Appl. Phys. 23 (1952) 779.
[109] H.T. Davis, J. Am. Ceram. Soc. 60 (1977) 499.
[110] F. Gritti, G. Guiochon, Anal. Chem. 78 (2006) 5329.
[111] F. Gritti, G. Guiochon, AIChE J. 57 (2011) 346.
[112] F. Gritti, G. Guiochon, AIChE J. 57 (2011) 333.
[113] D. Hlushkou, S. Bruns, A. Hotzel, U. Tallarek, Anal. Chem. 82 (2010) 7150.
[114] E. Wilson, C. Geankoplis, J. Ind. Eng. Chem. (Fundam.) 5 (1966) 9.
[115] S. Khirevich, A. Daneyko, A. Höltzel, A. Seidel-Morgenstern, U. Tallarek, J. Chromatogr. A 1217 (2010) 4713.
[116] A.S. Moharir, Chem. Eng. Commun. 11 (1981) 377.
[117] C. Dewaele, M. Verzele, J. Chromatogr. 260 (1983) 13.
[118] G. Carta, J.S. Bauer, AIChE J. 36 (1990) 147.

[119] F. Gritti, G. Guiochon, J. Chromatogr. A 1166 (2007) 30.
[120] F. Gritti, G. Guiochon, J. Chromatogr. A 1216 (2009) 1353.
[121] F. Gritti, G. Guiochon, J. Chromatogr. A 1166 (2007) 47.
[122] F. Gritti, G. Guiochon, Anal. Chem. 81 (2009) 3365.
[123] F. Gritti, G. Guiochon, Anal. Chem. 81 (2009) 3365.
[124] F. Gritti, G. Guiochon, Anal. Chem. 80 (2008) 6488.
[125] F. Gritti, G. Guiochon, J. Chromatogr. A 1206 (2008) 113.
[126] F. Gritti, G. Guiochon, J. Chromatogr. A 1217 (2010) 1485.
[127] F. Gritti, G. Guiochon, Chem. Eng. Sci. 65 (2010) 6310.
[128] F. Gritti, G. Guiochon, J. Chromatogr. A 1217 (2010) 5069.
[129] K. Kaczmarski, J. Kotska, W. Zapala, G. Guiochon, J. Chromatogr. A 1216 (2009) 6560.
[130] K. Kaczmarski, F. Gritti, J. Kotska, G. Guiochon, J. Chromatogr. A 1216 (2009) 6675.
[131] F. Gritti, G. Guiochon, Anal. Chem. 75 (2003) 5726.
[132] F. Gritti, G. Guiochon, Colloid J. 71 (2009) 480.
[133] K. Horvath, F. Gritti, J. Fairchild, G. Guiochon, J. Chromatogr. A 1217 (2010) 6373.